MODELING THE AUTOIGNITION, COMBUSTION AND POLLUTANT FORMATION IN A HIGH-SPEED DIRECT INJECTION DIESEL ENGINE

BY

RAHMAT I SHAZI

B.Sc., University of Manchester Institute of Technology

THESIS

Submitted in partial fulfillment of the requirements
for the degree of Masters of Science in Mechanical and Industrial Engineering
in the Graduate College of the
University of Illinois at Urbana-Champaign, 2002

Urbana, Illinois

ABSTRACT

With ever increasing challenge in meeting emissions standards dictated by countries, engine manufacturers are turning to computer models to help predict engine performance. In order to reduce pollutant emissions, engines have to sacrifice some efficiency. By understanding the basic combustion processes, we further our knowledge into the physics behind actual phenomena in our bid to gain some control over it. One technology that benefits from this research is diesel combustion.

Prior research has shown that an air-fuel mixture will autoignite given sufficient time and the right environment. Autoignition has been found to be a very complex phenomenon, with experimental work indicating there might be in excess of a thousand or more species responsible for it. This leads to the development of simplified models that capture the intrinsic fuel-air reaction that is the cause of autoignition. One of the models that have been developed is the Shell model. It has been applied with some success in modeling diesel engines. Along with this, the extended Zeldovich model has also been tested in its ability to model NOx production. With some modification and application especially into the KIVA code, both models are able to capture the general behavior of actual engines with some accuracy.

This research attempts to model the behavior of a high-speed diesel engine available at UIUC. It is a single-cylinder test engine modeled after the Ford DIATA engine planned as Ford's next generation hybrid vehicles' engine. The Shell model and the extended Zeldovich model are both inserted into the computer code KIVA-3V2 and the results are analyzed.

It was found that the code could predict the pressure trace hence the onset of ignition with reasonable accuracy. However, the NOx prediction is still not too close although the results are better than what has been obtained by previous researchers. The results also show that limiting value of switching temperature used to define start of combustion can be extended further from 1100K to 1150K. Obviously some work is needed to improve upon the code but the code is able to model the autoignition phenomena with good results.

ACKNOWLEDGEMENTS

I would like to thank first and foremost Prof. Chia-Fon Lee for his guidance all the way through this work. Although it has been difficult, I really appreciate his advice and patience in helping me tackle this research. The two years have been filled with ups and downs, but Prof Lee has always been there with advice that I'll cherish always.

There are a number of persons without whom this thesis would never have made it. First, I'd like to thank Dar-Lon Chang who assisted me in familiarizing myself with KIVA. He has been there all along to help me figure out concepts, errors, possible solutions and also discuss our personal lives. His presence has made the experience in UIUC very fulfilling. I am also indebted to Steve Chin for his files, codes and explanations as to his additions to the code. Others who have made an impact are fellow graduate students like Hatem Wasfy, Rajan Kapadia, DongYao Wang, Yi Xu, Tiegang, Jeremy Cellarius (without his experimental data, this thesis would have been moot), Will Matthews and Joshua Powell. A special thanks goes to Prof. Nick Glumac for his help during the tough first six months here in the States.

I would like to thank Universiti Teknologi PETRONAS, the main sponsor of my studies over in UIUC. Without the financial support, I would not find it so easy to pursue my dreams.

The support and understanding shown by my wife Azurawati Zaidi when it mattered most is greatly appreciated and will be treasured always. Thank you all.

TABLE OF CONTENTS

LIST OF FIGURES **Page**

CHAPTER 1

INTRODUCTION

For more than a century, the internal combustion engine as we know it have dominated the automotive power plant market. This has lead to a very great reliance on petroleum as a fuel source. While petroleum is currently reasonably priced, it is not renewable. The possibility of inflated prices once this commodity is scarce is a very real problem. A more serious concern today is the emissions from automotive engines, which is known to adversely affect the environment.

Internal combustion engines produce power by converting the chemical energy released by the combustion of fuel into mechanical energy, and in the process generating numerous by-products, many known to be hazardous to health, like carbon monoxide. This combustion process is influenced by a multitude of factors. One of these is the chemical reactions taking place inside the combustion chamber. Researchers have begun to understand that the reactions are not so straightforward as elementary chemistry makes it out to be. In fact, combustion reactions consist of hundreds or even thousands of reactions with similar numbers of chemical reactants. Trying to document these reactions are even more difficult given the randomness in which they occur and their dependence on other factors such as turbulence, spray atomisation and vaporization, chamber geometry and heat loss. Calculating the engine performance is thus very complicated when one tries to capture all actual processes taking place.

One method of simplifying these calculations is to model them using equations and relations. They are by no means the actual reactions taking place, but rather they capture the essence of all the chemistry and physical processes involved. This approach allows some insight into the behaviour of engines with respect to parametric changes. Sprays, vaporization and chemical reactions have all received this treatment.

Of course, all this would have been moot if it wasn't for the advent of the computer. The ability to do numerous calculations at great speed has allowed us to predict behaviour of actual systems. Although it is not perfect, this allows testing of new engine designs, new ideas for operating conditions, newly developed mathematical models and their validation compared to actual experimental results. Results from these models have been good so far, with the ability to capture actual engine trends and show how particular behaviour such as soot formation inside a diesel engine varies with changing parameters. Nowhere is this important than in diesel engines.

Why diesel? Diesel fuel is recognized as having greater energy density compared to gasoline. Its combustion mechanism is such that it offers higher theoretical engine efficiency and also fuel consumption. Diesel engines also have a higher compression ratio, which generally translates into greater torque. When one adds in the lower price of diesel, it is easy to understand why it is chosen for many heavy-duty and long rang transport applications.

Diesel engines have some drawbacks. Pound for pound, they are heavier than a similarly rated gasoline engine, as it has to withstand greater forces. The close-to-constant pressure combustion also leads to lower power output. A more serious problem though is its soot and pollutant emission. Due to the larger fuel molecules,

diesel engines tend to generate a lot of particulate matter (PM) through incomplete combustion. Older generation engines are notorious for emitting soot, but today that problem is being addressed by better combustion control and filtering. However, the generation of smaller particles, which are too fine to be clearly visible, has triggered more concern that these finer PM may pose even greater health risks. NOx generation is harder to control as the high temperatures so essential for the combustion of diesel it also the reason for its generation. Many methods meant to tackle NOx generation ends up boosting PM emissions. It is one of the most perplexing problems today, especially with many countries tightening the emissions standards for vehicles. Nowhere is this law tougher than in California, where the high vehicle density has caused health problems due to smog and other engine combustion products.

One difficulty in predicting diesel engine performance is caused by the autoignition processes inside the engine. Unlike gasoline engines where the ignition process is initiated by a spark, diesel engine ignition is caused by the exothermic chemical reaction inside the combustion chamber when fuel and air mixes at a very high temperature. Thus, the ignition process cannot be controlled directly. For this reason researchers have developed several autoignition models to predict how diesel fuel will combust. For the purpose of this thesis, the Shell model will be used exclusively to model it. It was initially developed to predict knock inside spark-ignited engines. The realization that knock and diesel autoignition is essentially the same process lead to its application in this neighbouring subject. It is not a simple single-step kinetic reaction but rather composed of several multi-step kinetic reactions that take place simultaneously. This increases its complexity, but can be easily tackled using computer simulation.

As pointed out earlier, engine manufacturers and researchers have several tools at their disposal to try and improve engine performance and emissions levels. One that is currently gaining lots of usage is the use of computer models. Complex mathematical models depicting the engine processes are fed into computers. The calculated results are shown as text data or even graphical images that allows users to visualize the simulated behaviour. By validating this data with actual measured ones, researchers can validate the model and try to pinpoint areas where the model may require refinements or a new approach altogether.

Prior to the development of computers, engine designers had to rely on actual experimental results as a performance yardstick. Engines had to be built and tested rigorously, and output data obtained using transducers. This setup is expensive since the manufacture of these engines and corresponding transducers able to withstand engine combustion forces required intensive labor. Any changes to engine parameters were time-consuming to say the least, especially if it involved changing chamber geometry. Even then, only vaguely qualitative data is available, like pressure trace, combustion images and general flow pattern. Discrete quantitative results are hard to obtain even using today's laser-imaging technology. This made engine testing and parameter changes laborious, but it was the only way of gauging the engine's performance. This is not only applicable to diesel engines, but to other heat-driven power plants as well.

With the advent of computers and mathematical models that simulate engine mechanisms and conditions, researchers can now design and test their engines using essentially mathematical experiments. Not only that, simulated numerical values at particular points in the computational grid can be obtained, which makes computational studies very useful. The models used to describe the engine needs to be

verified against experimental data, but the ability to model it gives great flexibility to engine designers to test new design ideas or operating schemes and have an idea how it will affect performance. Computational studies is also cheaper as it requires mainly computers and software, both which do not cost as much as building an actual engine.

It is with this hindsight that researchers start using computers to model diesel combustion. The complicated chemical reactions and physical processes, like spraying atomisation, heat transfer and soot formation can be modelled and applied to a particular engine geometry through the software. Available at UIUC is research software, KIVA-3V2 that has been heavily utilized for engine research. Part of its flexibility comes from the fact that users have access to its code, which is in FORTRAN. The ease of coding in FORTRAN but its ability to handle complex mathematical models has made KIVA-3V2 a very powerful engine simulation package. It can and has been used for other purposes as well. Improvements or new models can be substituted for the existing ones in this code, and the output can be configured to be read by a number of post-processors.

The existing KIVA software here at UIUC has been configured to include new models developed by previous graduate students. The main objective of this research work is to include the Shell autoignition model into this software and observe how it can better predict the operation of a single-cylinder diesel engine that has been tested at UIUC. This work also applies the extended Zeldovich model in order to calculate the rate of NOx generation in the hope of gaining better understanding of the mechanism and how it interacts with other parameters. This is hoped to give a better perspective on these models and how they help improve the prediction of engine simulation.

CHAPTER 2

LITERATURE REVIEW

Since Rudolph Diesel first introduced the diesel engine in the late19th century, a great deal of refinement and knowledge has been acquired on this engine through research and field tests. Initially, the diesel engine was meant to run using bio-diesel fuels, produced using plant oils as base material. But the arrival of cheaper petroleum made it even more attractive especially for heavy-duty applications. Good fuel economy and rugged reliability has made it invaluable for long distance transport applications.

However, the main disadvantages of the diesel engine compared to a spark-ignition engine have intrigued researchers looking for ways to reduce those effects. As mentioned in Chapter 1, the most obvious problems are the visible soot emissions and the lower power output per weight. Soot emissions are generated when incomplete combustion of the large diesel molecules in regions of high equivalence ratio i.e. rich regions creates coagulating carbon particulates. Their sizes depend on the combustion characteristics of the engine. This in turn is influenced by engine operating and characteristic parameters, like injection timing, geometry and turbulence. Researchers have developed and executed numerous experiments meant to shed more light on the topic. Some of the drive behind this research is the limit of knowledge we have about the actual phenomena taking place inside the engine. There is a great need to refine the understanding we have on the autoignition event.

2.1 Overview

Prior to the invention of the diesel engine, it has been noted that mixtures of fuel and air can ignite spontaneously if exposed to sufficiently high temperatures. The observation on spontaneous ignition has lead towards the idea that some exothermic reaction was taking place within the fuel-air mixture prior to the appearance of what we identify as combustion. These reactions supply the increase in internal energy needed to raise the temperature of the mixture that leads to the start of combustion. It has been seen that ignition in compression ignition engines are not instantaneous; a significant albeit short time delay exists between the establishment of the temperature and pressure required and the fast, exothermic chemical reaction we identify as combustion. The study into this delay is thus important in any application where spontaneous autoignition of fuel occurs. This delay is controlled by near-isothermal chemical reactions that take place before ignition, but we have limited knowledge into this phenomenon.

The spontaneous ignition of fuel-air mixtures invariably exhibits a time delay, and research has shown that the chemical reactions responsible for it are also responsible for knock in spark-ignition engines [1-3]. It is reasonable to suppose that the progress of these reactions accounts for part of the ignition delay. However, to study these reactions and correlate it with some known quantity requires some insight into the actual behavior of fuel-air mixtures. In atmospheric conditions, the chemical ignition delay is of the order of minutes and thus is easy to study. It is also easy to make observations as any reaction consequence can be observed. Initial work on the spontaneous combustion of fuel-air mixtures were done as early as 1906 by Falk [2] using a compression machine consisting

of vertical cylinders with weight-driven pistons. In his case, a mixture of hydrogen and oxygen was used, and the mixture was observed until combustion took place.

2.2 Experimental Studies and Observations on Autoignition

It is now generally accepted that knock is the ignition and combustion of a fuel-air mixture that is detonated due to the piston movement and expansion of burned gas. These phenomena compress the fuel-air mixture, causing it to heat up adiabatically until the point of combustion is reached without the direct influence of the approaching flame front [3]. Initially, because of the complexity of internal combustion engines, knock has been studied by isolating the autoignition process and observing it under low pressure conditions. Several experiments were done by using low pressures in gas bulbs [4], and at high pressures in rapid compression machines [5-9] and in motored engines [10]. These experiments showed some general pattern in the behaviors of fuel-air mixtures undergoing autoignition. Some of these behaviors include slow combustion, cool flames, single- and two-stage combustion.

Cool flames are defined as the exothermic process that precedes the hot ignition event. Under a cool flame, the temperature and pressure of the fuel-air mixture rises significantly. It is then quenched by the sudden decrease in the concentration of radicals as the temperature enters a region where the termination of radicals becomes significant enough to retard its growth. This is observed as a very noticeable reduction in temperature rise inside a chamber where such a mixture is kept. As time progresses, the temperature of this mixture will reach a point at which the molecules have enough internal energy to overcome the activation energy for combustion. When that happens,

hot ignition is said to occur. Figure 2.1 characterizes this. It shows how the temperature in a rapid compression machine varies with respect to time varies. The invisible scale on the left refers to species concentration. These species, R, B and Q will be explained later under the discussion of the Shell model.

Cool flames and the cool-flame stage of combustion reflect the self-quenching behavior of the reaction. The fast exothermic step was needed to bridge the gap between these phenomena and combustion. To know exactly the species involved in this reaction would be a very major step towards describing the autoignition phenomena. However, the work by Fish [4] showed that there were an enormous number of intermediates that take part in this phase of reaction. This was a major stumbling block in explaining knock properly.

Affleck *et al.* [8,9] carried out significant research work into autoignition. They studied results on compressing fuel-air mixtures in what is known as the Thornton Rapid Compression Machine (RCM) at the Shell Research Center in the UK. Back in 1968, the first paper on this machine was published explaining the operating mechanism [9]. Essentially it consists of a small 1.5" diameter cylinder and around 17" long. A piston is driven at high speed to compress a mixture of fuel and air. The machine has transducers and devices that allow it to sample the mixture composition at any particular instant and optical equipment that obtain photographic data of the combustion event. The pressure history is also recorded and is used as the primary data in many simulation studies, particularly ignition delay work. Figure 2.2 shows a layout of the components that make up this device.

The Thornton RCM results were important because it gave very accurate pressure and temperature data at the end of the compression stroke. Not only that, it also showed the two-stage ignition phenomena clearly on the pressure data obtained. Figure 2.3 shows the results of a typical experiment on the two-stage ignition of isooctane in a fuel-lean mixture (φ=0.9) with air. Trace ABCDE is the record of the gas pressure in the combustion chamber. The piston starts accelerating at point A and is brought to rest at point B in 10 ms. In that period, the fuel-air mixture has been compressed by a ratio of 9.6 to 1, and its temperature and pressure is 686K and 1.86 MPa respectively. Two-stage ignition can be seen in the subsequent pressure trace. A well-defined cool flame at D is seen increasing the pressure slightly but significantly, before the pressure trace settles into a slow increasing trend ending with abrupt ignition at E.

Figure 2.4 shows a one-stage ignition process that occurs at higher initial charge temperatures. In this case, the nitrogen in the air has been replaced by argon to decrease the mixture's specific heat capacity. The temperature and pressure at the end of compression is about 787 K and 2.12MPa respectively. Due to the higher initial temperature and pressure, the quenching of the cool flame is obscured by the steady exothermic reaction that is seen in a two-stage ignition.

The significance of this research is that it allowed us is to carefully measure and determine the expected behavior of fuel-air mixtures under knocking conditions. This was the primary reason for the development of the RCM, and also of the Shell model. By testing different fuel-air mixtures, different ambient conditions and different cell temperatures, a general picture of what takes place inside the combustion chamber is obtained. Through these observations, theoreticians began to formulate equations to

explain why the process of autoignition is observed. These experiments also showed six main features of autoignition that has to be modeled [11]:

i) a sharp, well defined two-stage ignition of a millisecond time frame, with the first and second induction periods around 0-30 ms

ii) a temperature rise during the cool flame rate of around 200K, with a rate of temperature rise of around 10^5 K/s

iii) rapid and complete quenching of the cool flame causing a close to zero temperature rise during an extended period prior to ignition

iv) rapid acceleration of the reaction rate after ignition event occurs

v) a transition to a single-stage from the two-stage ignition with an increase in initial and/or end-of-compression temperature

vi) a region of 'negative temperature coefficient' whereby the ignition delay increases with an increase in temperature

In addition, the model must be able to predict the changes in species concentration and its effect on the induction periods of autoignition. However, since the rate of fuel consumption is relatively low prior to the start of autoignition, this is a less stringent requirement.

From there onwards, several proposed theories were developed to describe this mechanism. These are in the form of mathematical equations that show that no matter how complicated the actual reactions are, the phenomological model and its complexity is not necessarily the result of the chemical complexity. This approach also takes into account all the significant chemical steps involved.

The Shell model comprises of a series of simultaneous chemical reactions that relate the change of species concentration to the heat evolved in the autoignition mechanism. The premise is that degenerate branching plays a crucial role in defining the cool-flame and two-stage ignition phenomena observed during autoignition of fuel-air mixtures. It models the autoignition process under the conditions of high pressure and temperature achieved in a rapid-compression machine or engines. What makes it very useful is that the originators successfully made it general enough for application to a wide array of fuels instead of just a few choice ones. Researchers are thus able to model anything from hydrogen to heavy diesel fuels. The equations are also reasonably simple for a model that simulated a complex interaction that probably involves more than 1000 species in the actual engine itself.

To begin with, Halstead *et al.* assumed that the chain-propagation cycle provides the skeleton for their model. Several steps that have a first-order dependence on the radical involved in the reactions propagate the reaction chain. To simplify analysis, all the radical concentrations are assumed to be in steady state in relation to each other, and is a good approximation especially if the propagation steps are fast compared to the branching and termination steps. For the chain cycle that involves i radical species, the reaction is written as:

$$r_1 \xrightarrow{k_{p1}} r_2 \tag{2.1}$$

$$r_2 \xrightarrow{k_{p2}} r_3 \tag{2.2}$$

$$r_n \xrightarrow{k_{pn}} r_1 \tag{2.3}$$

where $k_{p1}[r_1] = k_{p2}[r_2] \ldots = k_{pn}[r_n]$. In the generalized scheme, a single radical r_i will encompass all the radicals of the same type but of different detailed structure depending on the fuel complexity. In terms of the radical species, the concentration of any radical species r_i is given by

$$r_i = R/[k_{p_i} \sum_{j=1,n} (1/k_{p_j})] \tag{2.4}$$

where R is the total radical concentration. The term in square brackets is identified with an overall propagation rate coefficient, k_p, and will be dominated by the slowest step in the chain reaction. The concentration of radical r_i is then written as

$$[r_i] = Rk_p / k_{p_i} \tag{2.5}$$

Next, they assumed that the degenerate-branching agent, called B, is created by the dissociation of a single radical, r_i:

$$r_i \xrightarrow{k_j} B + r_j \tag{2.6}$$

where k_j is small compared to k_{pi}. The next assumption is that the branching agent dissociates into 2 unspecified radicals r_j:

$$B \xrightarrow{k_B} 2r_j \tag{2.7}$$

At high pressures and temperatures in an RCM or actual engines, the removal of radicals from the system is governed by homogeneous gas-phase processes [12]. This has not been identified experimentally, but Halstead et al in a later paper defined the termination reaction as the conversion of radicals into an inert species [16]. To properly model the termination steps, Halstead et al chose both a linear and quadratic termination rection that are incapable of propagating the chain. The reactions are

$$r_i \xrightarrow{k_t} out \tag{2.8}$$

$$2r_i \xrightarrow{k_{er}} out \tag{2.9}$$

To complete the model, the formation of radicals from the initial fuel-air mixture was also defined:

$$RH + O_2 \xrightarrow{k_q} 2r_i \tag{2.10}$$

Thus the complete Shell model is made up of eight reactions taking place simultaneously and competes for several species, and also temperature dependent.

Further development of this model took place between 1973 and 1977, when the next paper on the Shell model was published in 1977 [16]. The main difference here is that the propagating reactions' rate is defined to be fractions of the main propagating cycle's, k_p. The final notations used by Hallstead *et al.* are as follows:

Eqn 1: Formation of radicals R from fuel-air mixture:

$$RH + O_2 \xrightarrow{k_q} 2R \tag{2.11}$$

Eqn 2: The propagation step with heat evolved

$$R \xrightarrow{k_p} R + products + Heat \tag{2.12}$$

Note: The products generated are CO, CO2 and H2O in specific proportions. Heat evolved in this equation is calculated from the overall equation and was found to be 40 kJ per cycle of reaction.

Eqn 3: The propagation step generating B, the degenerates

$$R \xrightarrow{f_1 k_p} R + B \tag{2.13}$$

Eqn 4: The Propagation step generating Q

$$R \xrightarrow{f_4 k_p} R + Q \tag{2.14}$$

Eqn 5: The propagation step generating B through conversion of Q

$$R + Q \xrightarrow{f_2 k_p} R + B \tag{2.15}$$

Eqn 6: Degenerate branching

$$B \xrightarrow{k_b} 2R \tag{2.16}$$

Eqn 7: Linear termination of R

$$R \xrightarrow{f_3 k_p} out \tag{2.17}$$

Eqn 8: Quadratic termination of R

$$2R \xrightarrow{k_t} out \tag{2.18}$$

2.4 Results from Simulation Studies and Analysis

The Shell model has been applied with some success in modeling the autoignition process in spark-ignition and compression-ignition engines. Some modifications were required as per computer code utilized, but the general scheme was left almost unchanged. This section will look at some of these research studies to clarify any improvements made to this model.

One of the first attempts to model the autoignition process was done by the originators of the model, Halstead *et al.* In 1977 they published a paper [16] showing the complete Shell model and the simulated results obtained from a zero-dimensional model applied to the Thornton RCM in an attempt to curve-fit the values of constants associated

with the model. A reasonable degree of agreement with experimental results was obtained. In their studies, it was found that the concentration of Shell species R, B and Q varied with respect to time with clear indication of the cool flame phenomena and its quenching. This is implied in the sudden drop in the concentration of R indicating heat release associated with a cool flame. The quenching of the flame is defined by the leveling off in the concentrations of R. The second induction period is then characterized by the time lag between the end of the cool flame and the start of hot ignition. By curve-fitting they published a table defining the values for the Shell model constants matched to 100 RON, 90 RON and 70 RON fuels. This is shown in Table 2.1 in Appendix C.

Figure 2.5 shows the results of their investigation in 1977 into the temperature and its effects on induction periods and cool flame intensity for the autoignition of isooctane. There are regions of 'negative temperature coefficient', where the total ignition delay increases with increasing initial temperature. This is an important aspect of autoignition that any model must capture to be of use.

One of the first applications of the Shell model was by Natarajan and Bracco [17]. For verification purposes the Shell model was applied to the modeling of the Thornton RCM and constant-volume bomb experiments. After verification, it was then applied to the modeling of knock inside a gasoline engine. In their simulations, because of limitations of the REC software used, and the inability of the Shell model to be applied to a 2-D model due to mass imbalance among other things, they concentrated on comparing the trends computed with two limits observed experimentally, the Ignition criterion and the Inhibition criterion. The former relates to the way flame acceleration affects the low–temperature chemistry associated with the Shell model which in turn feedbacks into the

flame acceleration. The latter looks at how the flame propagation inhibits the low-temperature reactions and hence is not affected by them. Their results indicates that knock is better modeled using the inhibition criterion instead of the ignition criterion, the former which captures the different flame behavior under different knocking conditions.

Schäpertons and Lee [18] made the next contribution by defining the termination species for the Shell model. Previously, it was assumed that the termination of radicals generate no products since there are only trace amounts to begin with. This paper instead maintains mass balance by assuming that the radicals are turned into inert nitrogen molecules. For the linear termination step, Eqn (2.17) becomes:

$$R \xrightarrow{f_3 k_p} \frac{MW_R}{MW_{N_2}} N_2 \tag{2.19}$$

while the quadratic termination reaction, Eqn (2.18) is now :

$$2R \xrightarrow{k_t} 2\frac{MW_R}{MW_{N_2}} N_2 \tag{2.20}$$

They also combined the unbalanced propagation reactions into a single propagation reaction that maintains mass balance. The improvements are through the combination of Eqns (2.12), (2.13) and (2.14) into:

$$R + (\Lambda + 1)(\frac{1}{m} RH + pO_2) \xrightarrow{k_p} qP + f_1 B + f_4 Q + R \tag{2.21}$$

where $$\Lambda = (f_1 MW_B + f_4 MW_Q)/(\frac{MW_{RH}}{m} + pMW_{O_2}), \tag{2.22}$$

with MW denoting the molecular weight of the species in subscript. As with other species, the new species R,B and Q must be included in the conservation equations for

mass, momentum and energy in order to properly account for spatial distribution and transport. To account for the all other variables that completes this modification:

- fuel RH: fuel structure is C_nH_{2m} sets MW_{RH}

- products P: with λ as CO_2/CO ratio and

$$\frac{1}{m}RH + pO_2 \longrightarrow qP \tag{2.23}$$

- where $\lambda = 0.67$, $p = \frac{n(2-\lambda)+m}{2m}$, (2.24)

$$q = \frac{n}{m} + 1, \tag{2.25}$$

$$MW_P = \frac{\frac{n}{m}\lambda MW_{CO} + \frac{n}{m}(1-\lambda)MW_{CO_2} + MW_{H_2O}}{q} \tag{2.26}$$

- radicals R: from Eqn (2.11):

$$MW_R = \frac{MW_{RH} + MW_{O_2}}{2} \tag{2.27}$$

- branching agent B: from the reaction $B \longrightarrow 2R$,

$$MW_B = 2MW_R \tag{2.28}$$

- labile intermediate species, Q: from Eqn (2.15),

$$MW_Q = MW_B \tag{2.29}$$

Initial simulation with these modifications using the software REC-P3 showed some problems pertaining to predicted temperature and branching agent concentration.

The predicted peak pressure at combustion is too low, peaking at only 1150K. Significant oscillations in the concentration of B predicted were also seen right before hot ignition. As it turns out, the amount of heat evolved was inadequate to properly model ignition, and a modification was made by increasing it by a factor of Λ+1. Another change was to freeze the reaction rates at 950K regardless of local cell temperature, which helps stabilize the concentration of B right before combustion. Figures 2.6 and 2.7 shows a comparison of how these changes made the simulated results closer to expected trends during combustion.

With the advent of faster computers, more useful improvements to the Shell model could be implemented and more options could be explored. A number of papers have been published by Kong *et al.* at the University of Wisconsin-Madison showing the successful implementation of the Shell model into the software KIVA-II. The model is able to predict the onset of autoignition and achieve a very close match to experimental data. One of their studies [20] has great importance because it effectively shows that the model is very sensitive to the parameter A_{f4} that controls the rate of production of labile intermediates through the dissociation of radicals. As a matter of fact, their studies show that for application in common diesel engine simulations, values of A_{f4} several orders of magnitude than the original value defined by Halstead has to be used in order to obtain the right ignition delay. Figure 2.8 shows an example of A_{f4} variance on ignition delay as studied by Kong *et al.* [21].

A new development on the Shell model was published in 1999 by Sazhin *et al.* [22]. In this paper, Sazhin showed how by the substitution of the time differential in Eqns

The predicted peak pressure at combustion is too low, peaking at only 1150K. Significant oscillations in the concentration of B predicted were also seen right before hot ignition. As it turns out, the amount of heat evolved was inadequate to properly model ignition, and a modification was made by increasing it by a factor of $\Lambda+1$. Another change was to freeze the reaction rates at 950K regardless of local cell temperature, which helps stabilize the concentration of B right before combustion. Figures 2.6 and 2.7 shows a comparison of how these changes made the simulated results closer to expected trends during combustion.

With the advent of faster computers, more useful improvements to the Shell model could be implemented and more options could be explored. A number of papers have been published by Kong *et al.* at the University of Wisconsin-Madison showing the successful implementation of the Shell model into the software KIVA-II. The model is able to predict the onset of autoignition and achieve a very close match to experimental data. One of their studies [20] has great importance because it effectively shows that the model is very sensitive to the parameter A_{f4} that controls the rate of production of labile intermediates through the dissociation of radicals. As a matter of fact, their studies show that for application in common diesel engine simulations, values of A_{f4} several orders of magnitude than the original value defined by Halstead has to be used in order to obtain the right ignition delay. Figure 2.8 shows an example of A_{f4} variance on ignition delay as studied by Kong *et al.* [21].

A new development on the Shell model was published in 1999 by Sazhin *et al.* [22]. In this paper, Sazhin showed how by the substitution of the time differential in Eqns

9-12 with the change in the molar concentration of fuel. This improvement increases the accuracy of species prediction in the whole mechanism. However, the implementation of this model is not considered for this thesis, but more details can be found in [22].

The Shell model has been laid out here. It is essentially a simple multi-step kinetics model that predicts the presence of pseudo-species that compete to achieve autoignition. It will be applied to the simulation of a high-speed diesel engine, but as we shall see, numerous modifications have to be made in order for this model to predict the actual engines behavior. However, none of the changes are major and keeps the equations very close to the original scheme as developed by Halstead back in 1973.

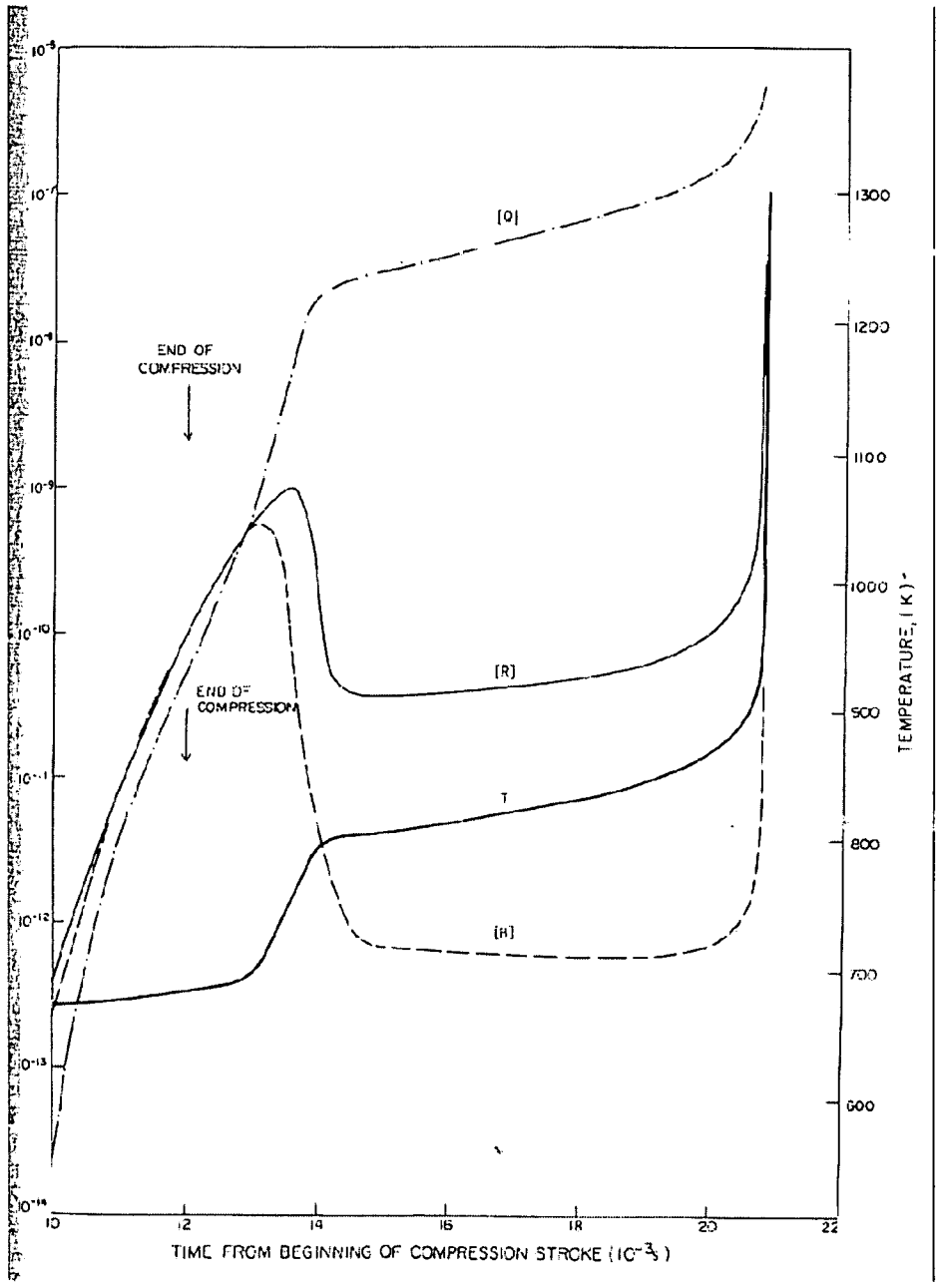

Fig 2.1: Typical simulation of two-stage ignition in the Thornton rapid compression machine [16].

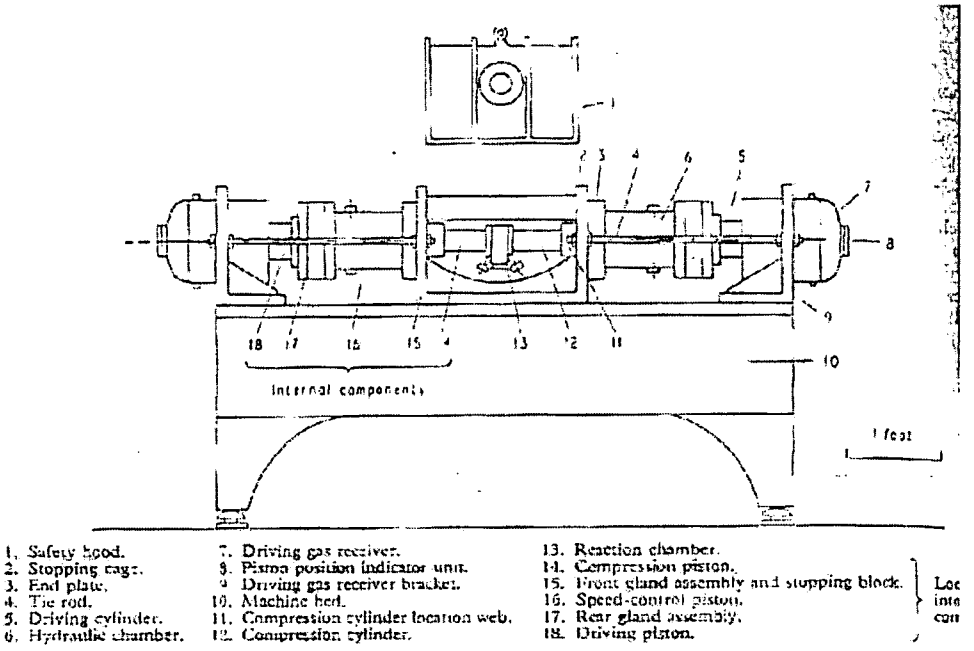

Fig 2.2: Layout of the Thornton rapid compression machine major components. [8]

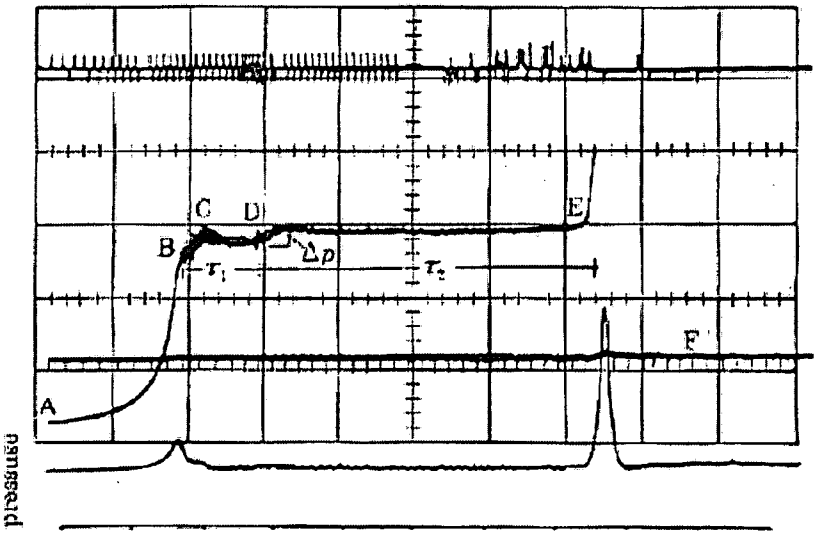

Fig 2.3: Typical oscilloscope records of autoignition of a 0.9 stoichiometric mixture of isooctane in a rapid-compression machine. Trace shows a two-stage ignition at a pressure of 1.86Mpa and 686K. [12]

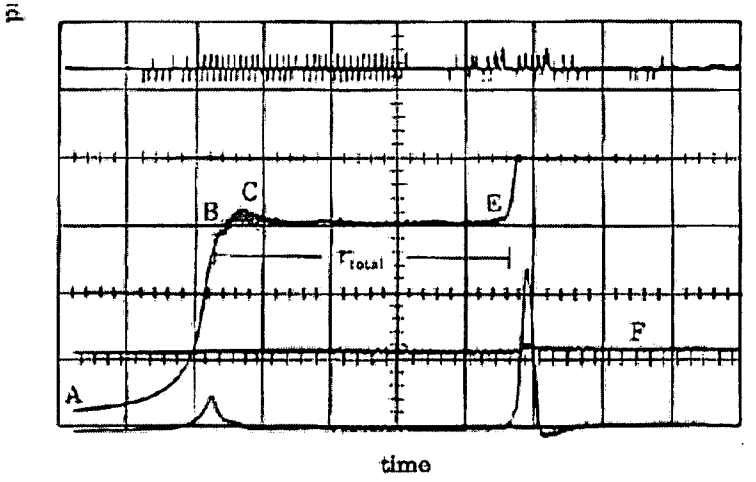

Fig 2.4: One-stage ignition at higher initial temperature. [12]

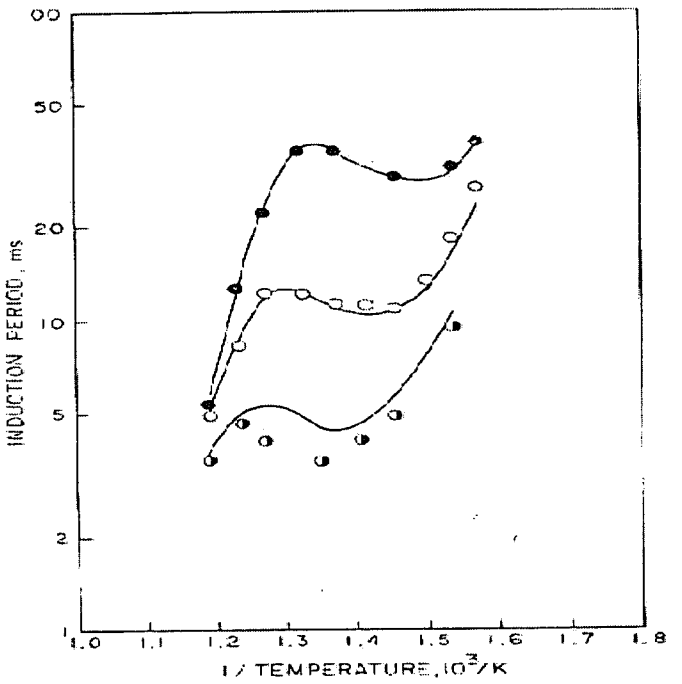

Fig 2.5: Plots of ignition delay in the RCM with variations in fuel.RON, top is 100 RON, center 90 RON and lowest data point corresponds to 70 RON The simulation input parameters are: a compression ratio of 9.6, wall temperature 373K, 0.9 stoichiometric mixture. Lines are simulation results while symbols are experimental data.[16]

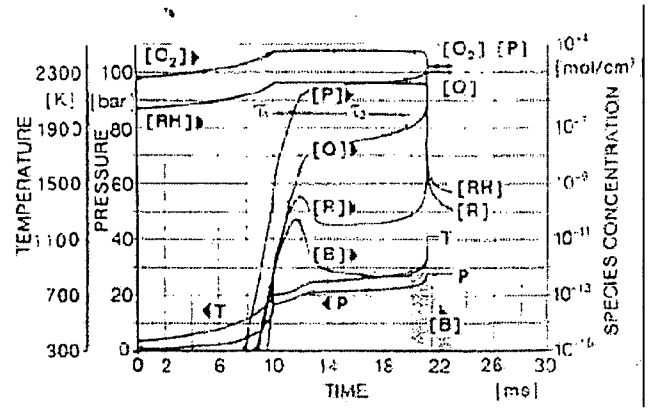

Fig 2.6: Pressure, temperature and concentrations during RCM computation, preliminary case [18]

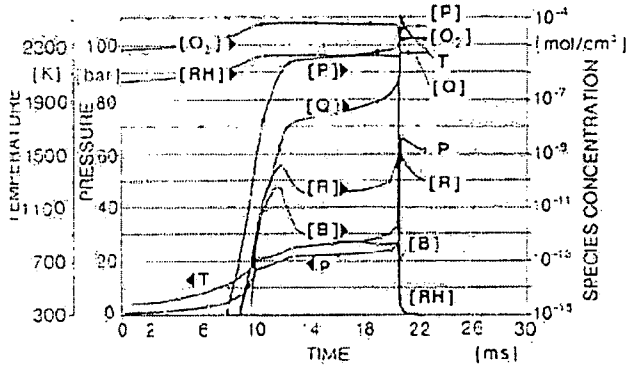

Fig 2.7: Pressure, temperature and concentrations during RCM computation, modified case [18]

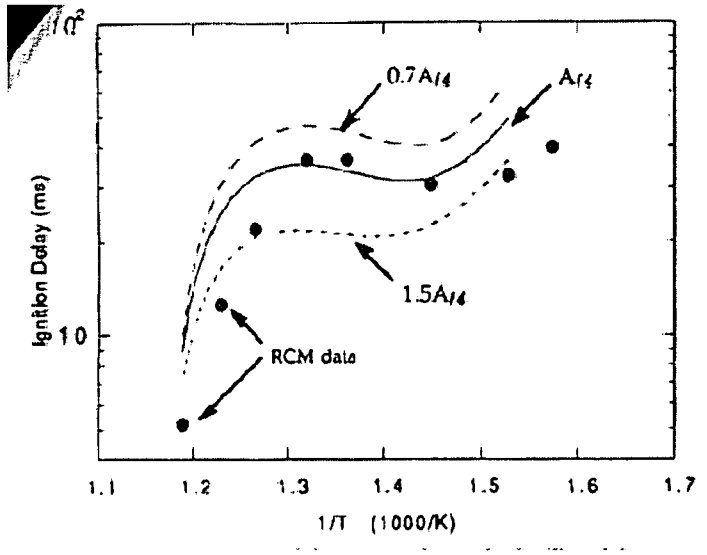

Fig 2.8: Effect of A_{f4} on ignition delay as applied to the RCM simulation

CHAPTER 3

KIVA AND IMPLEMENTATION OF THE SHELL MODEL

The first computers were designed to do complicated calculations that would have taken top mathematicians years to solve due to the nature of the equations describing the problem. The need for repetitious calculations without error opens up the feasibility of using computers as a primary tool of research instead of being support equipment. Nowhere in research is this being realized as much as in the simulations of actual physical situations. With development of new software and matching hardware, computers are used to model anything from river flows to nuclear explosions. It has also found a niche in performing calculations to predict the behavior of automotive engines.

That being said, a simulation is only as good as the input code. The dependence on actual experimental data is still of paramount, as it gives a guide for computer models to match. Not only that, experimental data allows the development of a new model or improvements to an existing one to be carried out.

However, a computer simulation has several advantages over the traditional approach of doing experiments. Not only is it more mobile, being dependent only on the availability of a code and a computer to run it on, it is also much cheaper. A typical experimental setup may cost thousands of times the price of a computer and software. It is also much easier to obtain quantitative results, compared to many invasive and non-invasive techniques employed in experimental work. It is through the use of computers

that many engine R&D departments could cut down time and money spent on development on new engines. This translates into better products at a lower cost and hence better competitiveness. All of the major car manufacturers utilize computer models extensively for this reason.

In the research community, a number of software has made their mark. Names like REC, KIVA, STARCD are all well known to the engine modeling person. For computational research here at the University of Illinois, the software KIVA is readily available and is used to test new models of fuel sprays, pollutant formation, droplet vaporization and combustion. It is this software that is used in this particular research into engine autoignition.

3.1 General Outline of Software

The Los Alamos National Lab released the first version of KIVA in 1985. It is designed to calculate transient three-dimensional dynamics of fuel spray, evaporation, mixing of fuel-air mixtures, ignition, chemical reactions and heat transfer [23-25]. It has also undergone some changes through the years and these are documented in new manuals [26-28]. The code is written in Fortran, which although is not the most advanced computer language today, has been updated significantly. A major plus for Fortran is the relative ease with which mathematical formulations can be added to the code. The latest version, KIVA-3V2 is the software used in this research. From now on any reference to KIVA will refer to this updated version unless mentioned specifically.

KIVA solves the unsteady equations of motion of a turbulent, chemically reactive mixture of ideal gases, coupled to equations for a single-component vaporizing fuel spray

[26]. Although the equations are coupled, the code itself is modular and can be modified. Options and models can be altered, switched off or changed by new input to the source code. This flexibility allows researchers to test new equations or updates to the existing ones and observes how much of an improvement would be obtained in the result. Table 3.1 in Appendix C is a list describing some of the general capabilities of KIVA.

Much like other computational fluid dynamics (CFD) codes, KIVA solves the equations based on the finite volume method called the ALE (arbitrary Lagrangian-Eulerian) method. A finite-difference mesh subdivides the computational region into a number of smaller cells that are hexahedrons. The corners of the cells are vertices and their positions are arbitrarily functions of time. The mesh can conform to various shapes to match the contours of a combustion chamber.

The Cartesian components of the velocity vector are stored at the cell vertices, but during the computational cycle cell-faced velocities are used. This reduces the need for a node coupler, which the original ALE method depends on. The transient solution is obtained over a finite number of time increments called timesteps. On each cycle the variables are calculated from those of the previous cycle. Each cycle is divided into two phases – a Lagrangian and a rezone phase. In the first phase, the vertices move with the fluid velocity, and there is no convection across cell boundaries. In the rezone phase, the flow field is frozen, the vertices moved to new specified positions and the flow field is rezoned onto the new mesh.

As pointed out earlier, KIVA is highly modular. It consists of many files, some incorporate models, some incorporate the main body of the program and some acting as data files. There are at least 60 subroutines and in excess of 10000 lines of code in the

program. However, it is actually relatively easy identifying which subroutine handles a particular phenomenon to be modeled. For ease of identification, input files of KIVA tend to begin with the letter I whilst all output files begin with the letter O. Hence the file OTAPE8 is an output, whilst ITAPE7 is an input file.

In order to define the computational domain in KIVA, the user can utilize a mesh-generator program, K3PREP. This mesh generator reads in the geometrical characteristics of the mesh to be modeled through the input file IPREP and generates the mesh accordingly. The mesh file is an output file OTAPE17, which is renamed to ITAPE17 for it to be read by the KIVA executable. The operational parameters for the engine or mesh are entered through the input file ITAPE5. This distinction has to be made as KIVA, although was developed for the engine community, has the flexibility to be modified for numerous different applications, such as droplet vaporization and formation. More details on KIVA can be obtained in references [23 -28]. However for the application of the Shell model, the subroutine that is most important is ***chem.f.***

The subroutine ***chem.f*** includes the kinetic reaction model for KIVA. Many chemical reactions that takes place will be handled by about 600 lines of code in this subroutine, more if necessary. It simulates the kinetics reactions especially through the oxidation of fuels during combustion, the production of pollutants and others. The subroutine calculates the reaction rate based on the equations and the basic time-variation equation of species that's described by the differential equation:

$$\frac{d[i]}{dt} = \sum \{(\upsilon_i'' - \upsilon_i')) \times k_j \times \prod_{l=1}^{L} [i]^{\upsilon_i'} \} \qquad (3.1)$$

with i = index of species

j = index of reaction

l = index of reactants in reaction j

L = number of reactants

N = number of reactions

υ' = stoichiometric coefficient for reactants

υ'' = stoichiometric coefficient for products

More information on how ***chem.f*** handles the chemical kinetics is explained in Appendix I of reference [25], and Appendices B and C show the input files' codes.

One of the drawbacks of the subroutine is that it is designed to handle only single component fuels and only simple straightforward single step kinetic reactions. It has to be modified significantly in order for it to model the multi-step kinetics of the Shell model. Not only that, the Shell model itself is easily applicable for zero-dimension calculations, but the equation for fuel concentration as shown earlier will not work in a multidimensional model due to the motion of species through the multiple cells defining the computational domain. Some modification is thus required.

3.2 Addition of Shell Model

One of the first steps in the application of the Shell model to ***chem.f*** is to define the rate of production of species to be a competition between several equations. The Shell model, as recommended by the several references [16-22] is switched on only in cells with a local temperature of less than a varying value between 950 to 1100K. This value is defined as the switching temperature, defined as *tcut* in the input file ITAPE5. It is meant

to serve as the main instigator of ignition through the exothermic reaction as mentioned in Chapter 2. Above this temperature, combustion occurs.

To facilitate the switch between the two models, the approach taken is to have two main code blocks in ***chem.f***. The first block handles any kinetic reactions that happen below the switching temperature or *tcut*, specifically the Shell model, and the second block handles the combustion part of the model.

One of the initial parts of modification work to the present chemical kinetics routine is to develop the block of codes to handle the Shell model. Instead of generating a new subroutine, it was decided to instead develop the new block within ***chem.f*** instead. Since the codes for the basic chemical kinetics were already in place, that particular block was used as a template for the Shell model as opposed to writing a new code from scratch.

The second phase was calculating the reaction rate constants according to Halstead et al. This involved the addition of new data to the code and the definition of new variables for the concentrations of species involved i.e. fuel, oxygen, radical R, intermediates Q and branching agent B, products P and the formation of nitrogen. The full form of the Shell model was discussed in Chapter 2. From these reactions, differential equations defining the production and conversion of the Shell-specific species R, B and Q can be written. The differential equations defining the rate of species change are as follows [16]:

$$\frac{1}{V}\frac{d[R]}{dt} = 2\{k_q[RH][O_2] + k_B[B] - k_t[R]^2\} - f_3 k_p[R] \tag{3.2}$$

$$\frac{1}{V}\frac{d[B]}{dt} = f_1 k_p[R] + f_2 k_p[Q][R] - k_B[B] \tag{3.3}$$

$$\frac{1}{V}\frac{d[Q]}{dt} = f_4 k_p[R] - f_2 k_p[Q][R] \tag{3.4}$$

The rate of oxygen consumption is defined by this equation :

$$\frac{1}{V}\frac{d[O_2]}{dt} = -pk_p[R] \tag{3.5}$$

Halstead defined the rate of fuel used by this equation:

$$n_{RH} = \frac{(n_{O_2} - n_{O_2}\{t=0\})}{pm} + n_{RH}\{t=0\} \tag{3.6}$$

A differential equation defining the temperature rise of the mixture was also developed, very important during the times of zero-dimensional analysis. The equation is written as:

$$\frac{dT}{dt} = \frac{1}{C_v n_{tot}}(Q_K - Q_L - \frac{n_{tot} RT}{V}\frac{dV}{dt}) \tag{3.7}$$

where Q_K is the chemical heat release defined by the equation:

$$Q_K = k_p qV[R] \tag{3.8}$$

and Q_L is the heat loss through the boundary walls defined as:

$$Q_L = \phi V(T - T_W) \tag{3.9}$$

with ϕ the product of the heat transfer coefficient and the surface to volume ratio of the chamber in question. Details of these equations can be found in [16]

The rate constants for Eqns (3.2-3.8) are defined by the following expressions:

$$f_1 = A_{f1}\exp(-E_{f1}/RT)[O_2]^{x1}[RH]^{y1} \tag{3.10}$$

$$f_2 = A_{f2}\exp(-E_{f2}/RT) \tag{3.11}$$

$$f_3 = A_{f3} \exp(-E_{f3} / RT)[O_2]^{x3}[RH]^{y3} \tag{3.12}$$

$$f_4 = A_{f4} \exp(-E_{f4} / RT)[O_2]^{x4}[RH]^{y4} \tag{3.13}$$

$$K_i = A_i \exp(-E_i / RT) \tag{3.14}$$

where i include p_1, p_2, p_3, q,b and t with the exception of K_p :

$$K_p = \frac{1}{\frac{1}{K_{p1}[O_2]} + \frac{1}{K_{p2}} + \frac{1}{K_{p3}[RH]}} \tag{3.15}$$

which represents the reaction rate of the main propagating step, Eqn (2.12).

Next was the discretization of the time-variation for Shell-specific species. As originally defined, the equation will work for a zero-dimensional simulation but has to be modified in order to work in a three-dimensional simulation.. Based on the updated Eqn (2.23), the rate of consumption of fuel is now defined as:

$$\frac{d[RH]}{dt} = -\frac{1}{m} Kp[R] \tag{3.16}$$

This is based on the assumption that since the rate of oxygen consumption is dependent on radical concentration, by the same token so must fuel concentration, which only reacts with oxygen according to Eqn (2.11). Note also that Eqn (3.7) is not used as KIVA already has a more advanced subroutine to calculate the temperature variation, which is more comprehensive than the simple form defined by Halstead. A final addition is the rate of production of products, P. Instead of converting it into the individual components of CO, CO_2 and H_2O, Schäpertons opted to leave them as P. However, no equations have been defined in the previous publications. It is uncertain whether this omission is intentional or accidental. The rate of production of P is given by the equation:

$$\frac{d[P]}{dt} = q\,Kp[R] \tag{3.17}$$

which is also derived from Eqn (2.23).

To complete the list of equations for the Shell model, an expression for the exothermicity of main propagation reaction has to be defined. From Eqn (3.8), the amount of heat evolved is defined as:

$$Q_K = (\Lambda + 1)\,q\,K_p\,V[R] \tag{3.18}$$

This completes the Shell model as it is applied in ***chem.f.***

3.3 NO formation: the Extended Zeldovich model

Diesel engines are notoriously known for the soot that their exhaust emits. Less visible but just as harmful is the amount of oxides of nitrogen that can form inside the combustion chamber at the high pressures and temperatures required for autoignition. The principal source of NO is the oxidation of atmospheric nitrogen. The inclusion of an NO formation model will be most helpful to allow for the prediction of pollutant production from an engine. For this research, the Extended Zeldovich model has been adopted.

The reaction mechanisms governing the formation of NO from molecular nitrogen are [32]:

$$O + N_2 \longleftrightarrow NO + N \tag{3.19}$$

$$N + O_2 \longleftrightarrow NO + O \tag{3.20}$$

$$N + OH \longleftrightarrow NO + H \tag{3.21}$$

The forward and backward reaction rates are given in Table 3.3. From these equations, the rate of formation of NO can be simplified [29] to the following equation:

$$\frac{d[NO]}{dt} = \frac{6\times10^{16}}{\sqrt{T}}\exp(\frac{-69{,}090}{T})[O_2]_e^{1/2}[N_2]_e \qquad (3.22)$$

where the subscript e denotes the equilibrium concentrations for the reaction denoted by Eqn (3.19). Therefore for implementation into the code, the equilibrium concentrations of oxygen and nitrogen have to be calculated in order for the Zeldovich model to be applied. However, instead of taking that approach, it was decided to utilize ***chem.f***'s existing code, which calculates species concentration change instantaneous concentrations, yielding a more accurate result. Through the use of Eqn (3.1), the time-variance of the species involved in the Zeldovich model are:

$$\frac{d[NO]}{dt} = k_{3.19}^{+}[O][N_2] + k_{3.20}^{+}[N][O_2] + k_{3.21}^{+}[N][OH] - k_{3.19}^{-}[NO][N] - k_{3.20}^{-}[NO][O] - k_{3.21}^{-}[NO][H] \qquad (3.23)$$

$$\frac{d[N]}{dt} = k_{3.19}^{+}[O\ ][N_2] - k_{3.20}^{+}[N][O_2] - k_{3.21}^{+}[N][OH] - k_{3.19}^{-}[NO][N] - k_{3.20}^{-}[NO][O] - k_{3.21}^{-}[NO][H] \qquad (3.24)$$

$$\frac{d[O]}{dt} = k_{3.19}^{+}[O][N_2] - k_{3.19}^{-}[NO][N] - k_{3.20}^{-}[NO][O] \qquad (3.25)$$

where the subscript denotes the equation, and the superscript denotes whether it is the forward (positive) or backwards (negative) reactions' rate of reaction coefficient.

3.4 Validation of Code: the Thornton Rapid-Compression Machine

In order to validate the code, some comparisons between its predictions and experimental results are required. Many references [17,18,20,21] use the Thornton RCM data as one of their validation cases. It was elected to do the same for this research work.

The Thornton RCM device, as explained earlier, is essentially a cylinder in which a mixture of fuel and air is rapidly compressed to a fix volume i.e. compression ratio. The device has a diameter of 1.5 inches and a usable compressible length of around 20 inches. Due to mechanical limitations at the time, the intended compression is achieved not by using one but two opposing piston accelerated simultaneously. This achieves the same effect but with less stress on the components, allowing easier motion and position control. By changing the stroke of the piston, various compression ratios can be achieved. A quartz window allows the direct visual observation of autoignition processes occurring inside the chamber.

Figure 3.1 shows the close up of the reaction chamber section. It shows the two opposing pistons at top-dead-center, the basic system arrangement for instantaneous sampling of chamber gas, and the quartz window used for visual inspection. It was and still is a very impressive and useful experimental apparatus.

To simulate this in KIVA, input parameters are defined in the file IPREP. Appendix B lists the input codes for the RCM case. Due to certain problems in the code, instead of forming a single block, the RCM mesh is generated using two blocks that are patched. The resulting mesh is very similar to one generated from a single block with no difference in computing accuracy. Similarly, instead of modeling two opposing pistons, the RCM is modeled using a single moving piston instead. This is accepted as the original

approach the RCM designers intended but could not achieve due to mechanical limits on the machine.

One of the main important parameters to get right is the motion of the piston as it accelerates down the cylinder. From the original paper [9], the displacement of the piston is shown in Figure 3.2. In order to simulate the motion in KIVA, the equation of piston position with respect to time has to be developed. To assist in this problem, the displacement data from the original paper is discretized and read into the software Kaleidagraph 3.5. This software has the capability to analyze a set of data and generate an equation that best fit it. In order to obtain the highest accuracy, the polynomial equation option is selected. Results from the process are shown in Figure 3.3.

The first attempts to simulate the RCM were made using a 2-D mesh, and the model parameters for 100 RON is used to avoid the need to define a multicomponent fuel in the testing period. Fuel amount is defined as 0.9 of a stoichiometric mixture due to the abundance in experimental data. Unfortunately, the simulation did not progress very far. Numerous error messages were obtained, indicating that there was some problem in the applicability of the Shell model as it is in 2D simulation. In view of this, 3D simulations were also attempted using a 60-degree axisymmetric mesh to observe for mesh dependence of the results. Initial conditions for the RCM simulation are set at 98 kPa initial chamber pressure, with the wall temperature kept at 373K. These input parameter values are chosen as they are used extensively as the initial starting conditions for the experimental work.

The first objective before running the simulations is to determine the optimum grid size for accuracy and shortest computer time. To test this, several grids were used: a

coarse one (12x4x25), and a medium one (13x6x30) and a fine mesh (16x8x35). The induction periods τ_1, τ_2 and ignition delays are shown in the radar chart in Figure 3.4. These results show that the ignition delay for the medium and fine meshes collapse on top of each other. This indicates that the medium mesh is adequate for convergence of the solution without taking up too much computer resources.

Before finalizing the inputs to ITAPE5, accurate simulation is also dependent on the timestep of the calculations. They need to be small enough especially for chemical equations with characteristics times in the order of 1e-4 s. To test this, several runs are made with maximum timesteps set at 1e-4, 1e-5 and 1e-6 s. Results from these runs show that the timestep of 1e-4 is adequate in capturing the essence of the Shell autoignition model, as indicated by Figure 3.5.

For validation work, the variance of ignition delay is compared with:

i. End-of-compression temperature using 100 RON

ii. Initial pressure i.e. charge density using 100 RON

This choice was made as there is ample data on these cases. Not only that, since 100RON is pure isooctane, there is very little chance that a multicomponent characteristic might affect the results. Experimental data is obtained from papers by Halstead *et al.* and Kong *et al.* [16,20] and reintroduced here.

3.5 RCM Results

An abundance of data is available on the simulation of induction time inside the Thornton RCM with fuels of different qualities, namely 100, 90 and 70 RON. For

validation, simulation data is compared with experimental results obtained from references mentioned above. Figure 3.6 and 3.7 shows plots comparing the simulated and the experimental results using parameters of 100 RON.

At first glance at Figure 3.6 and 3.7, it seems that the Shell model can only predict the general trend but not match the experimental data closely. However, similar differences are observed in the papers using the Thornton RCM as a validating case. According to Kong *et al.* and Schäpertons *et al.* [18,20], there are several possible main reasons for the difference that does not undermine the effectiveness of the model. They are:

i. Different heat transfer model compared to the actual experimental conditions.

ii. Variation in specific heat could be represented by a different model or different polynomial [30] used in modeling

iii. Different actual temperatures experienced by the cells. Experimentally, ignition is being defined as a function of the end-of-compression temperatures. However, it has been found [31] that the autoignition event is controlled by the increase in core gas temperature. At any particular point, the average temperature of the cylinder is probably lower than the central core, which means that ignition delay will probably be shorter than expected, hence the lower-than-experimental values.

iv. Inherent differences between the zero and multidimensional model [20]

As suggested by Kong et al., the kinetics scheme itself is expected to be qualitatively correct in terms of its two-stage ignition and most importantly, negative temperature coefficient. However, non-homogeneity of the cylinder temperature causes different rate of heat transfers and this affects the prediction.

A much better match is obtained with variance in initial pressure. This translates into variation in fuel concentration. This match seems expected, since the Shell model depends on the fuel concentration to generate radicals needed to propagate the reactions. There is a slight variance especially values of the second induction period, probably due to the difference in defining the end of the first induction period. Schäpertons *et al* [18] also found a similar difference in their research work. Experimentally, this is determined on the sudden decrease in pressure trace. But computationally, this is determined from the start of a decline in concentration of radicals. The difference in these approaches will lead to a difference in the ignition delay obtained.

The Shell model has been added to the KIVA-3V2 software and validated with respect to results obtained in the Thornton RCM experiments. It will now be applied to the modeling of the high-speed direct injection diesel engine in the hopes that it will be able to model the autoignition observed. The next chapter will present some basic outline of the engine. The basic methodology and results of this application is then presented in Chapter 5.

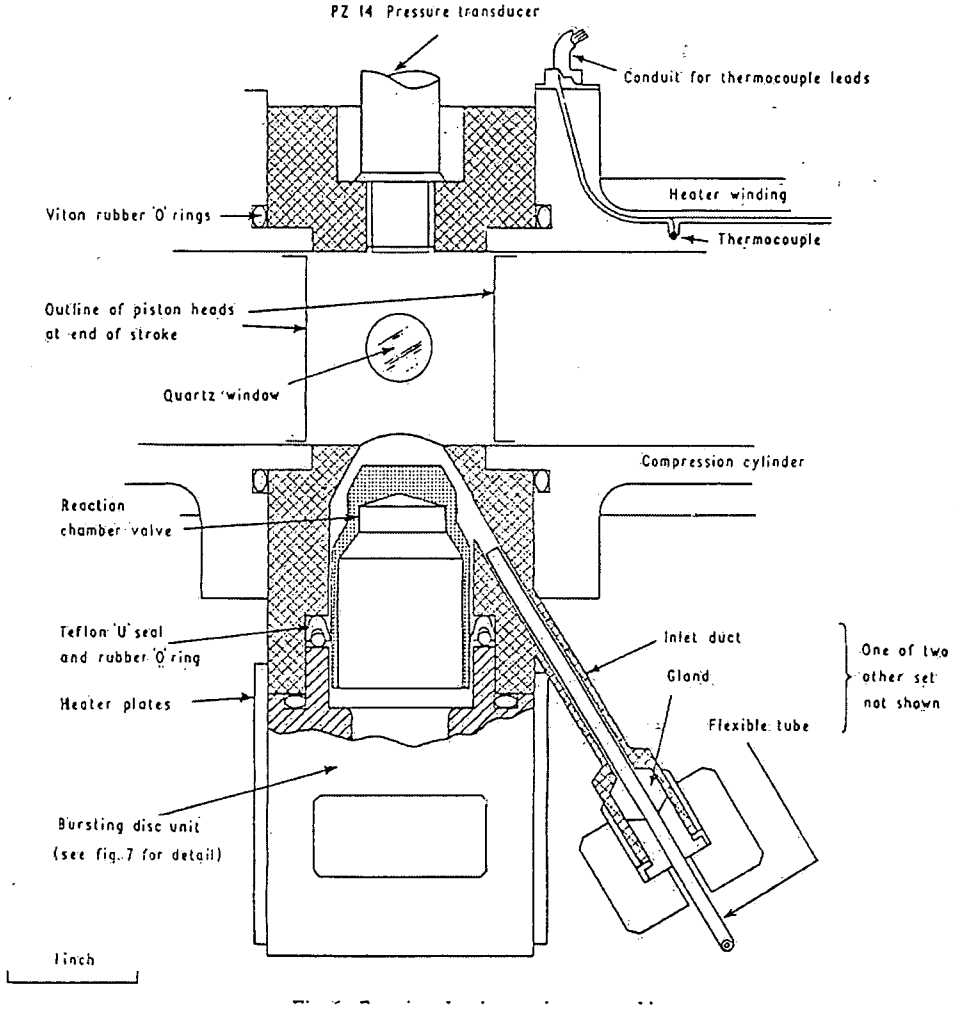

Fig 3.1: Reaction chamber section in Thornton RCM [9]

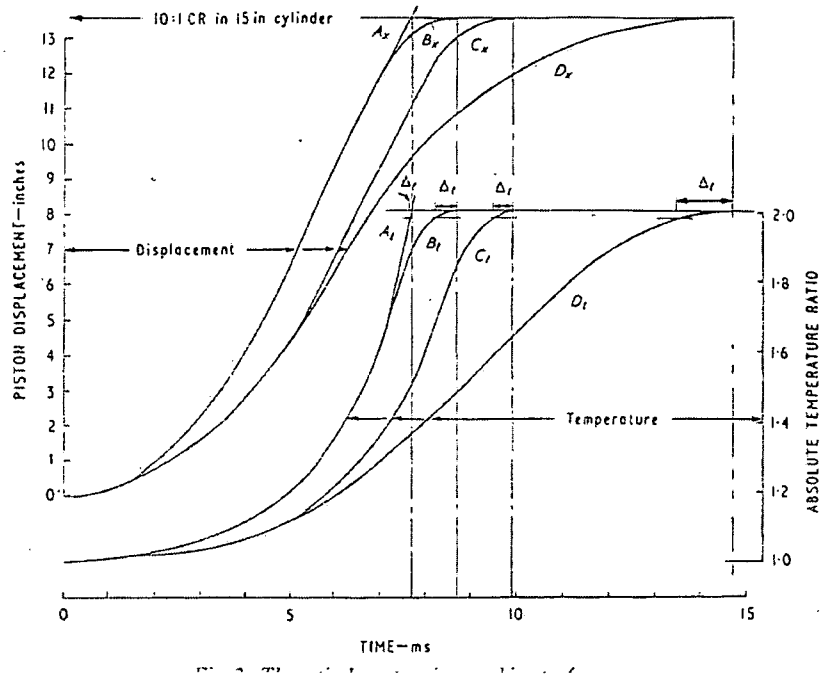

Fig 3.2: Theoretical RCM performance. Curve C_x is the desired motion, but in practice the piston stops at time=12ms [9].

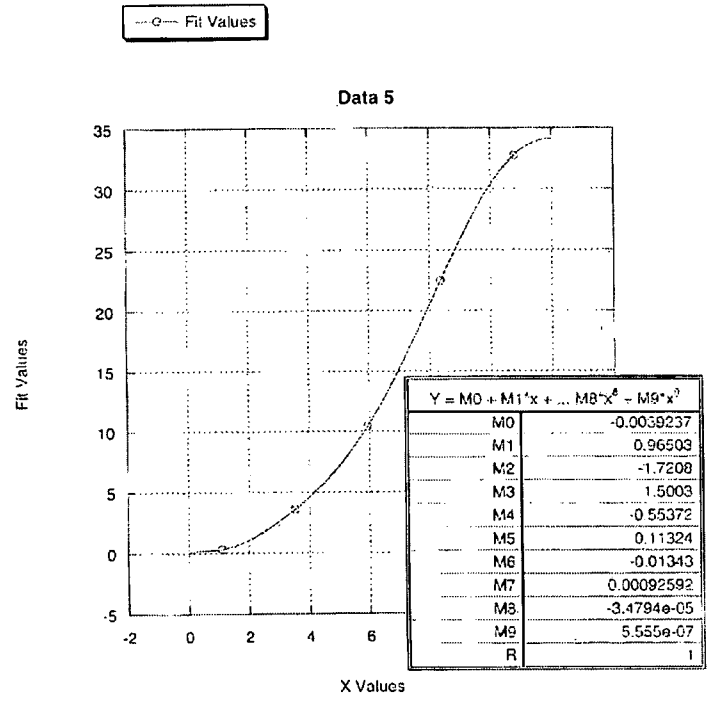

Fig 3.3: Plot of piston motion, discretized, and polynomial constants describing motion with respect to time.

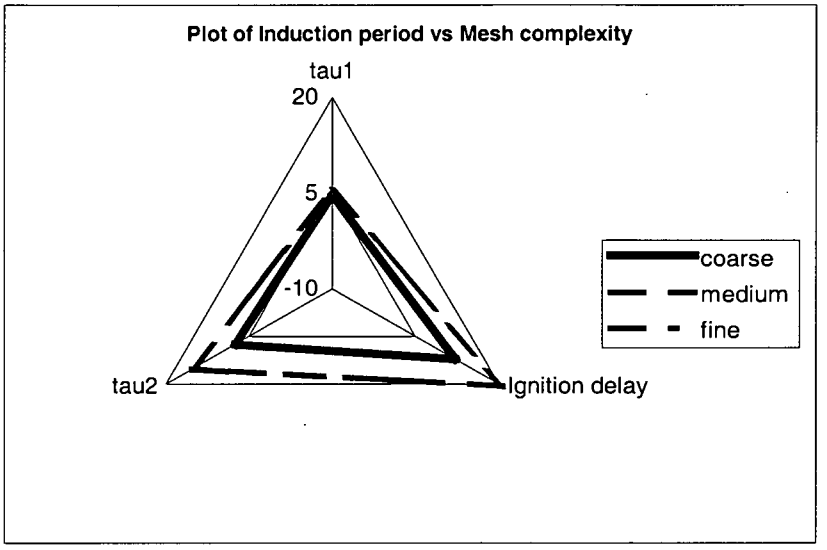

Fig 3.4: Radar chart shows results for fine and medium mesh collapses on top of one another.

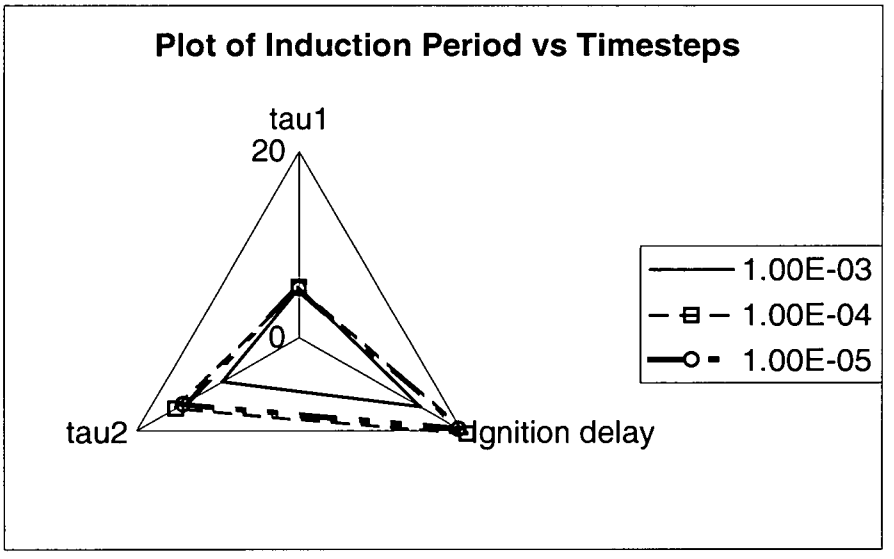

Figure 3.5: Radar chart showing induction period with respect to timestep changes.

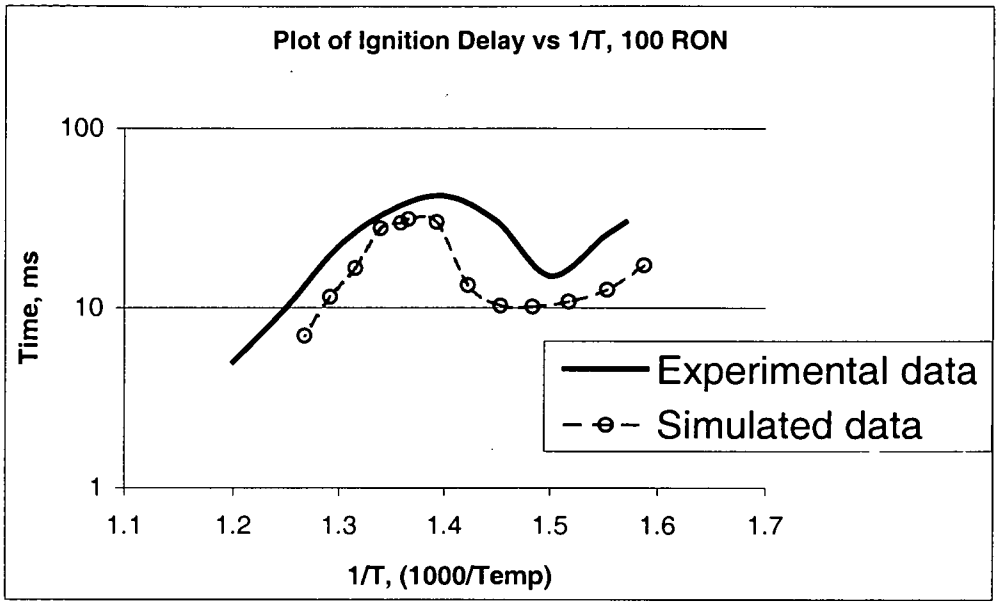

Fig 3.6: Experimental vs simulated data for ignition delay using 100 RON fuel

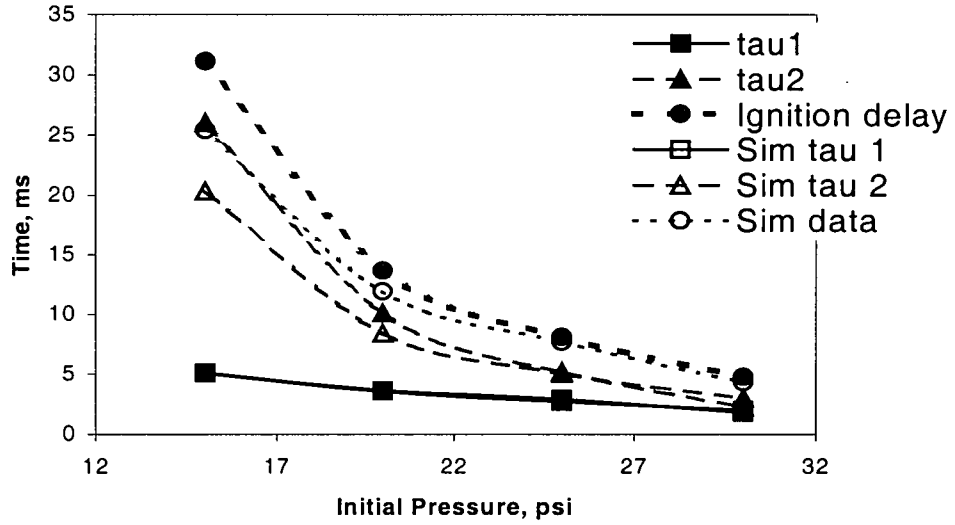

Fig 3.7: Experimental vs simulated ignition delays with the induction periods compared. Solid symbols are experimental data, open symbols are calculated using KIVA, fuel 100RON.

CHAPTER 4

THE HIGH-SPEED DIESEL ENGINE

The numerous advantages diesel engines have over gasoline-fueled ones become less obvious when the application demands power and speed. Most diesel engines have been tailored for heavy-duty application where low fuel consumption, great torque and reliability is required. Part of the problem has to do with the fact that combustion inside diesel engines are not directly controlled but rather is governed by the characteristics of the fuel-air mixture and the reactions leading to autoignition. The best a designer can do is to understand how operating parameters affect the in-cylinder operations, like injection timing, port timing, swirl ratio and so forth.

One of the challenges in producing a passenger car's diesel engine is the reduction in efficiency as the engine size decreases. Not only that, but for a good power range it has to run at a much faster speed. With smaller combustion chambers, the amount of time available to ensure good mixing of this heavy fuel is reduced thus leading to generally poor oxidation of fuel that causes dark soot to be emitted. Compared to gasoline engines, it has a lower specific power output due to the heavier construction required to endure greater stresses associated with high compression ratios. Any further improvement in diesel combustion will require a greater in-depth understanding of fuel-air mixing and autoignition processes.

Diesel engines have been used for passenger applications, but it was never very popular in the US due to stringent pollutant laws. The European market on the other hand has accepted it for some time. Only recently has the diesel engine been embraced especially in regions where gasoline costs more. In Asia for example, diesel is at least half the price of gasoline. A significant reduction in exhaust emissions has also made it viable as the new passenger car powerplant. Ford has identified that this particular engine may have a future as a hybrid car powerplant. It developed the DIATA (Direct-Injection, Through bolt Aluminum) engine specifically for this purpose. Here at UIUC, experimental research using a single-cylinder engine patterned after this design has been on-going for some time. There are significant amount of experimental data available, but for this research, emphasis will be put on the pressure trace and pollutant formation data.

4.1 Engine Descriptions and Experimental Data Obtained

The DIATA engine is a high-speed direct injection (HSDI) diesel engine with components made from aluminum as a way to reduce the mass of the engine. It has a bore of 70mm and a stroke of 78mm, with a compression ratio of 19.5. The piston bowl helps in generating swirl meant to assist in fuel breakup and vaporization, and provide the space needed for fuel introduction while allowing the squish region to be as minimal as possible. It is also designed to operate at much higher speed than typical large diesel engine. Speeds can reach up to 4000 rpm or more. A list of the basic specification of a single-cylinder research engine based on the DIATA is shown in Table 4.1 in Appendix C.

A ghosted view of the engine viewed from the top is shown in Figure 4.1. Experimental results from the engine were obtained from Jeremy Cellarius who collected the data from the engine for his MS thesis. The pressure trace obtained will be used as the primary guide for model matching. Other available data are NO concentration in exhaust and particulate amount. All experimental results are shown in comparison with the simulated data in the next chapter.

In Cellerius's work, the main parameters that were varied were:

i. Injection Timing: Four injection timings were used: 16.5 degrees BTDC, 9.5 degrees BTDC, 5.5 degrees BTDC, and 3.5 degrees BTDC

ii. Fuel amount: 7 mg or 10 mg of Tetradecane was injected

iii. Swirl Ratio: With one intake port activated/deactivated, swirl ratio is either 2.5 or 4.0

iv. Injection Pressure: Fuel was injected at either 600, 800 or 1000 bar. This parameter is not studied in this work, but is merely used to calculate the estimated spray velocity. Only injection pressure of 800 bar is used.

The simulation work will concentrate on the first three parameter variations and will disregard item iv. Simulation results will be compared to these available experimental data:

i. Pressure trace

ii. NO generated

The simulated results will be compared to the experimental data available from Jeremy Cellarius, and the discussions will be presented in the next chapter.

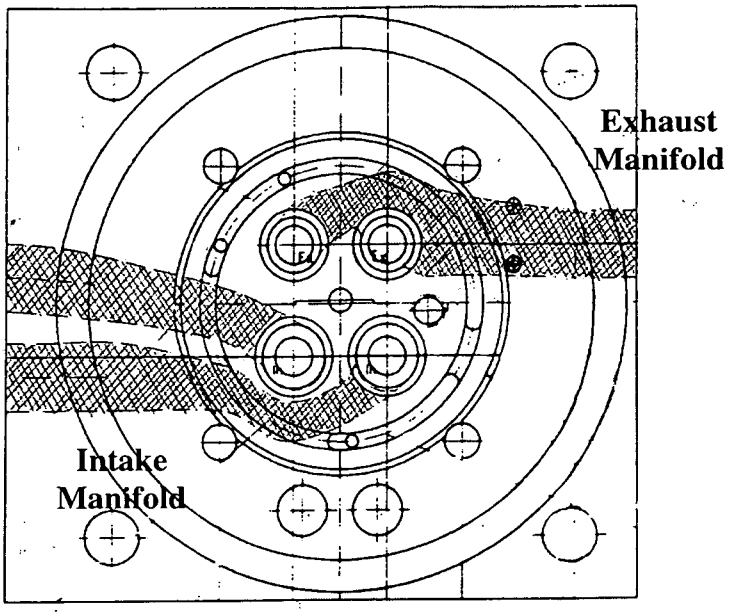

Fig 4.1: Ghosted view of the top of the HSDI engine

5.2 Input Parameters and Simulation Procedures

To cut down on computation time, the simulation was divided into two runs. The first run models the motoring condition up to 340 or 350 degrees crank angle. This allows for the simulation to complete calculations a few crank angles before injection starts. Any changes in the model or parameters associated with the Shell model can be inserted later. It also allows for the input parameters to be adjusted, accounting for the unknowns that might affect pre-injection pressure.

KIVA allows the user to include a large number of options for simulation flexibility. All operational inputs can be defined in the input file ITAPE5, or if needed, be included into the code. For this case, most of the inputs are defined through ITAPE5 similar to that shown in Appendix A. This chapter will discuss only the most important ones.

Experimental data show that the intake air was at 98 kPa and 300K. The walls of the engine are defined to be at a constant temperature of 400 K. The fuel spray was modeled using the preferential vaporization model developed by Y. Zeng *et al.* [30]. This model is already included into the current code available in UIUC. The computations used tetradecane ($C_{14}H_{30}$) to simulate the diesel fuel used in the experiments. It is expected that the engine will have some residual exhaust gas in the combustion chamber, which will increase the energy content of air at the start of a stroke. It was found that in order to match the pressure before injection, the input temperature has to be set at around 400~420K. Because of random irregularities, each injection timing case needs a different initial temperature. Work done has shown that a value of 412.7K gives a reasonable pressure match to all cases up to and at 10 degrees BTDC.

For the injection situation, initial work was carried out in modeling four baseline cases of injection timings: 16.5 degrees, 9.5 degrees, 5.5 degrees, and 4.5 degrees BTDC. For this simulation work, the amount of fuel injected is set at 7mg. The swirl ratio is set at 4.0. Unfortunately, the 16.5 degree case encountered numerous problems at start of injection, probably due to some coupled effect during the complex model of breakup and vaporization. It was thus discarded; instead attention is concentrated on the three remaining cases. From now on, the three cases are referred to as Cases A, B, and C respectively.

Combustion is set to occur in any cells with a temperature greater than 1150K by defining the value of the ITAPE5 input variable *tcut* as 1150. This was used because at lower values of *tcut*, early autoignition was observed. This pseudo-autoignition occurs because there are regions of high temperatures that exist inside the mesh. This value is not recommended by previous researchers [20,21]. The reasoning was that the values of the Shell model constants were not verified at temperatures greater than 1100K. However, as seen in Figure 5.3, temperatures inside the cylinder have exceeded 1100K. Setting the value of *tcut* below 1100K caused early ignition and skewed the results. The alternative solution for this simulation is to define the value of *tcut* to be greater than 1100K. After testing various increments in the value of *tcut*, it was found that a value of 1150K consistently and reliably exhibits the expected ignition delay. A good match with experimental data was also obtained; indicating that in this particular work, the 1100K limits defined by previous research can be pushed further.

5.3 Results

As stated in the literature review, the Shell model is known to be very sensitive to the constant A_{f4}. In order to facilitate easy modification, the input variable cf11 in ITAPE5 is configured to store the value of A_{f4}. This way, any changes to the model constant can be made in ITAPE5 instead of changing the value in chem.f. This reduces the need to recompile the code every time this value is changed.

Preliminary work done on Case B shows that the value of A_{f4} needs to be modified from the one given by the originators of the Shell model [16]. This modification was also done by Kong *et al.* [20,21] by varying this value to obtain the best possible experimental match. Figure 5.3 shows the best pressure match obtained is with A_{f4}=1e+4. Although this is a big change from the value defined by Halstead *et al.* [16], but in almost all the papers utilizing the Shell model [16-22] the value of A_{f4} is several magnitude larger. For example, Kong *et al.* in SAE 950278 used 1.3e + 6. This constant does depend on the grid as well.

A significant finding of this research is that shown in Figure 5.3. The research shows that a better match is obtained when the basic turbulent k-e model is used instead of the newer RNG k-e model. According to Kong *et al.* [21], this occurs because the RNG k-e model causes the fuel spray to evaporate faster. Spray penetration decreases as a result of using this model, and a much higher fuel vapor concentration are available for reaction. This leads to a shorter ignition delay, as shown earlier in Chapter 3 with the RCM case (Figure 3.9). As a consequence, the mixture autoignites sooner. Therefore the peak pressure in Figure 5.3 for the RNG k-e model is higher then the experiments. In this case, the more advanced RNG k-e model is not superior to the earlier k-e model.

Another option that is not switched on here is the laminar-turbulent mixing model. This laminar-turbulent mixing model increases the mixing rate between unburnt and burnt mixture, increasing the reaction rate. Figure 5.4 shows the pressure data associated with Case B. With this model switched on, the ignition occurs sooner but reaches the peak pressure slightly later compared with the data obtained with the model switched off. Therefore for the HSDI case, the best option is to switch both the laminar-turbulent model and the RNG k-e model off.

These options (Af4=1e+4, laminar-turbulent mixing model off, basic k-e model on) were initially applied to Case B. Again referring to Figure 5.3 shows the plot with experimental data for comparison. The simulated pressure trace shows a very good match with the results, especially when compared to the previous existing model in KIVA. The standard KIVA model suffers from too fast combustion during the early stages of combustion. This is the result of inadequate simulation of the low-temperature chemistry. Fast combustion causes fuel to vaporize quickly and prevent it from penetrating further into the combustion chamber. This results in low cylinder pressure during the expansion stroke. To verify this model, it was also applied to Cases A and C. Figures 5.4 and 5.5 shows the results with very good approximation.

To better illustrate these findings, some graphical results of in-cylinder distributions of temperature and other are shown. Figures 5.7 and 5.8 are both from Case B. They depict the temperature gradient inside the cylinder at TDC and 5 degrees ATDC. At TDC, the temperature inside the cylinder is barely high enough to cause combustion. Spray is still entering the cylinder, lowering the temperature at the center due to

evaporation. Five degrees later, there was still no sign that the ignition has taken place. The exothermic reaction associated with the radical conversion was still not observed. The central core temperature was still higher than 1100K, indicating that the previous ceiling of 1100K for tcut is not appropriate for modeling this high-speed diesel. Figure 5.9 shows that at 10 degrees ATDC, ignition occurs and combustion has taken place. This concurs with the experimental pressure that indicates ignition taking place around 8 degrees ATDC. The white central region slightly downstream of the injector nozzle has temperatures in excess of 2800K. This is probably the area where autoignition first takes place. There are still cool regions in the center, probably from the presence of fuel vapor. Assuming that the flame front is represented by the high temperature gradient seen in these images, we see that the fuel does not penetrate very far into the bowl of the piston

Unfortunately, the extended Zeldovich model is not as accurate as the Shell model in predicting the amount of NOx generated. As seen in Figure 5.10, the simulated NOx amount is far from the actual values. Patterson *et al.* [34] has discussed the factors that influence NOx prediction. It was found that the calculations are very sensitive to small changes in the computed in-cylinder gas temperature fields. Kong *et al.* introduced a calibration factor to match the experimental values, but with the standard k-e model it had to be set it at 62 to match experimental values i.e. the computed NOx was 62 times less than the measured data. In contrast, the current simulation overpredicts the measured data by about 2 to 3 times. This was not expected, as the standard k-e model was supposed to have under-predicted the NOx generated. The general trend of NOx formation with respect to injection time can be captured. With the proper calibration factor this model will probably be able to correctly predict NOx formation.

To further validate the code, a simulation of 10 mg of injected fuel at an injection timing of 5.5 degrees BTDC was made. The pressure trace is shown on Figure 5.11. It is obvious that without any changes in the model constants, the start of combustion in this engine can be modeled very well by the code for different load conditions and injection timings,

The Shell model and the extended Zeldovich model has been added to the software KIVA-3V2 to model the high-speed diesel engine. The results of the simulation shows good agreement with the experimental data, but the emissions model needs to be developed further to improve the utility of this model. It was found that the standard k-e model gives a better prediction over the RNG k-e model, which was unexpected but can be explained. The laminar-turbulent mixing model is also switched off as it causes the ignition delay to decrease significantly.

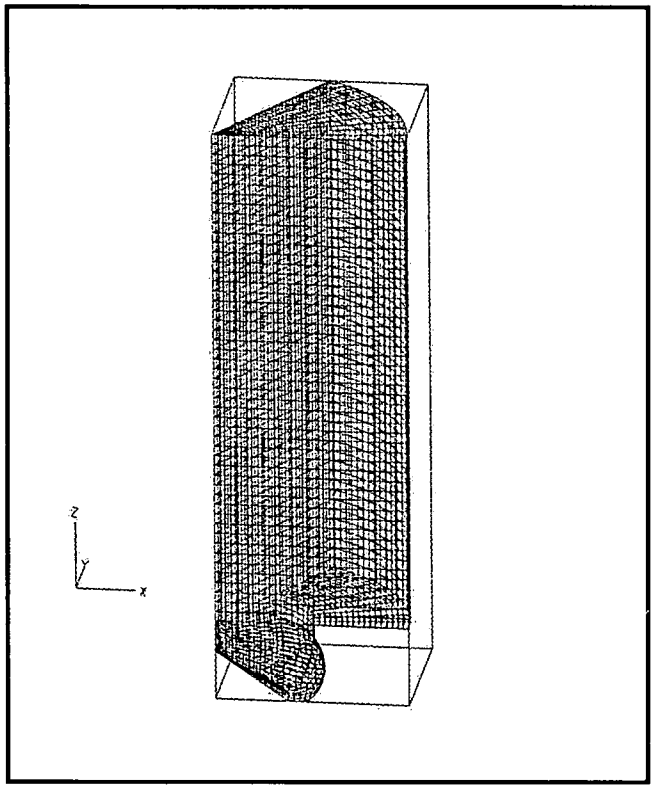

Fig 5.1: Diagram of the computational grid used for HSDI calculations

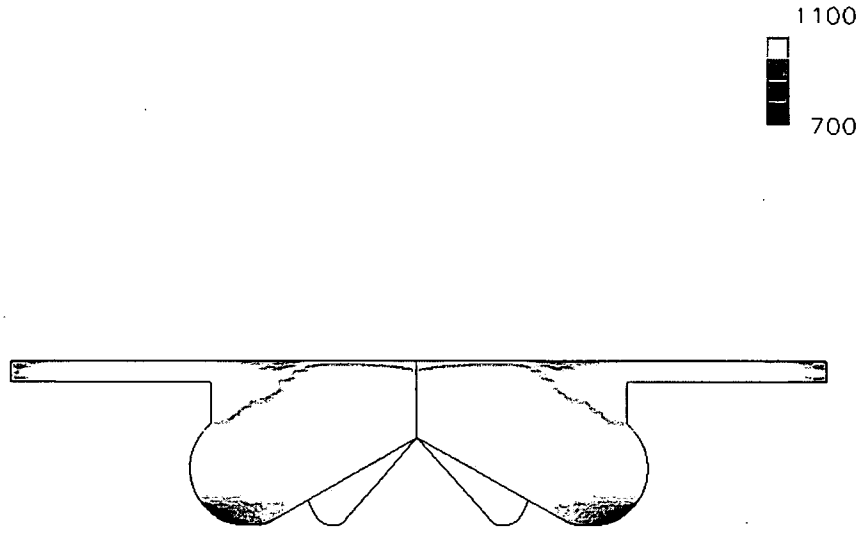

Fig 5.2: Black-and-white temperature distribution inside piston at 10 degrees BTDC. Notice the white region in the center indicating that the central temperature is greater than 1100K

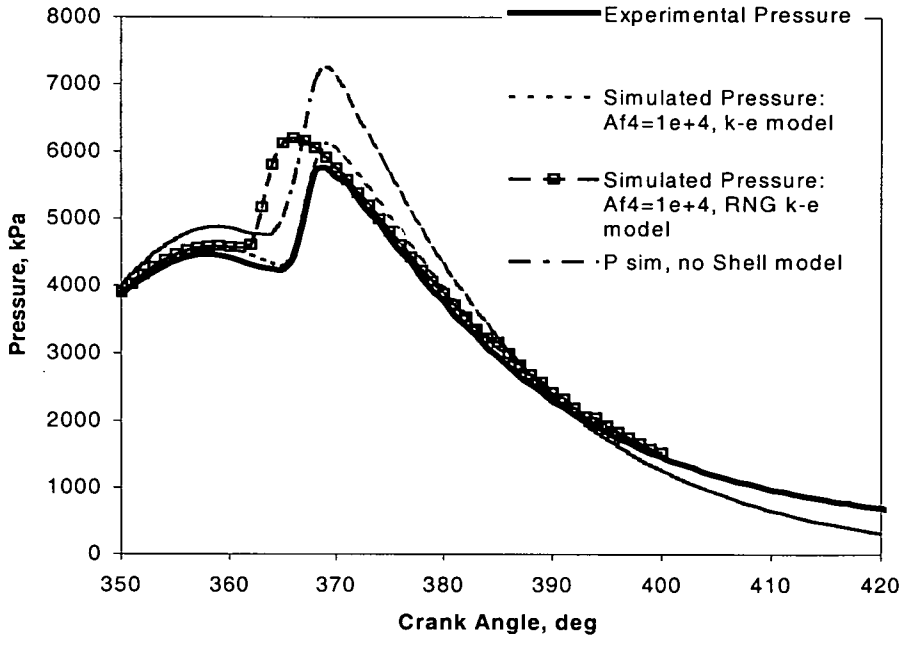

Fig 5.3: Pressure trace, experimental vs simulated for injection timing 5.5 degrees BTDC (Case B)

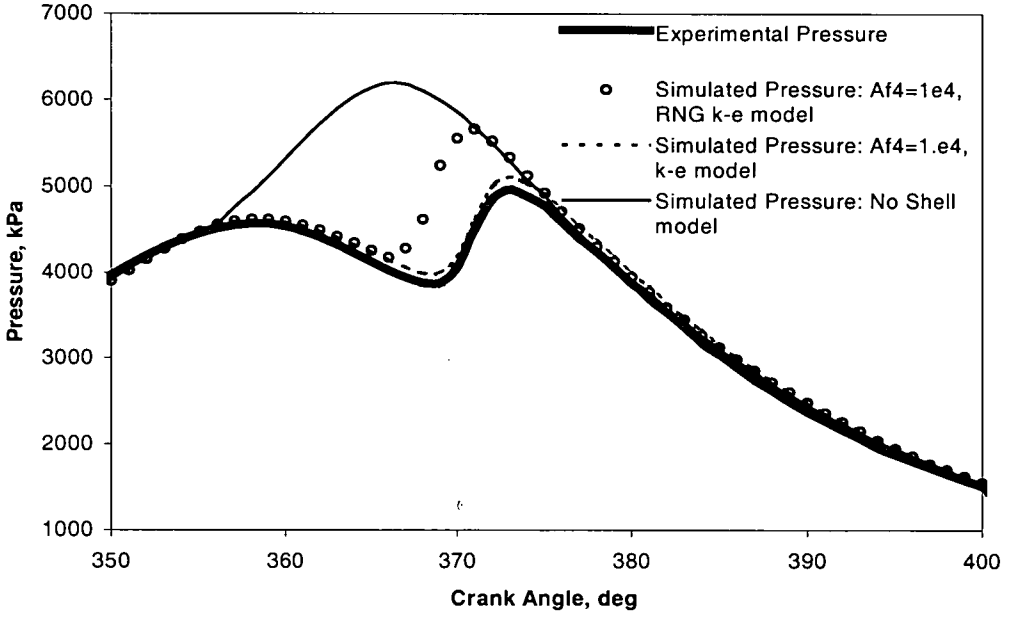

Fig 5.4: Pressure trace for Case C, injection timing 3.5 degrees BTDC

Fig 5.5: Temperature distribution at TDC, Case B

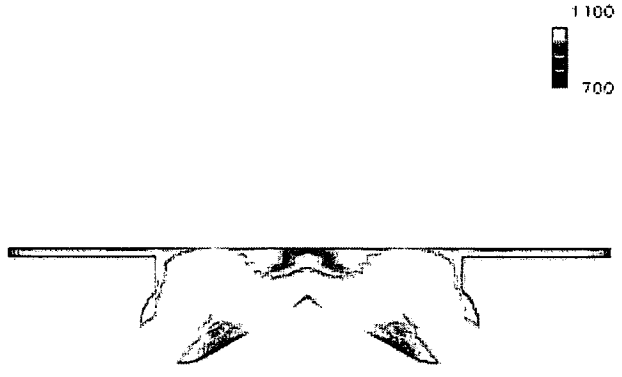

Fig 5.6: Temperature distribution at 5 degrees ATDC, Case B

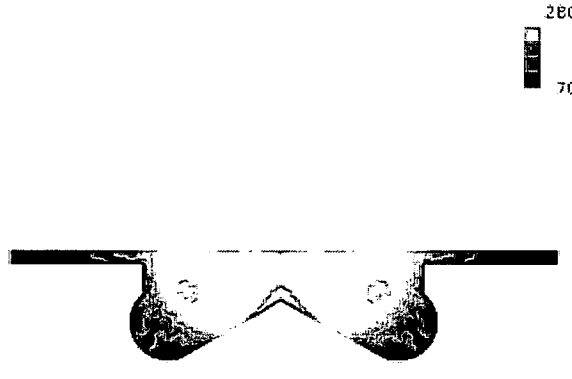

Fig 5.7: Temperature distribution at 10 degrees ATDC, Case B

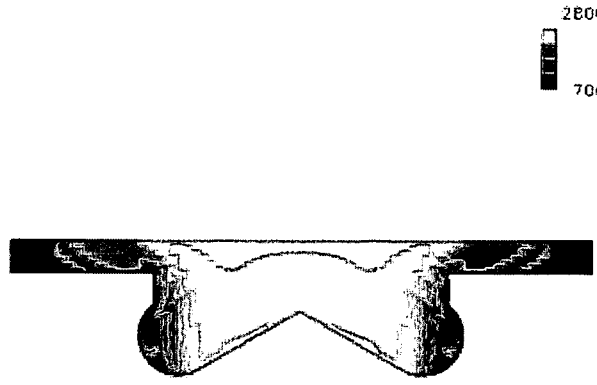

Fig 5. 8: Temperature distribution at 20 degrees ATDC, Case B

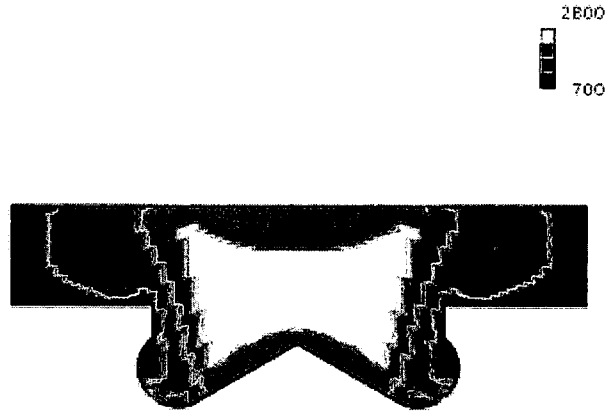

Fig 5.9: Temperature distribution at 20 degrees ATDC, Case B

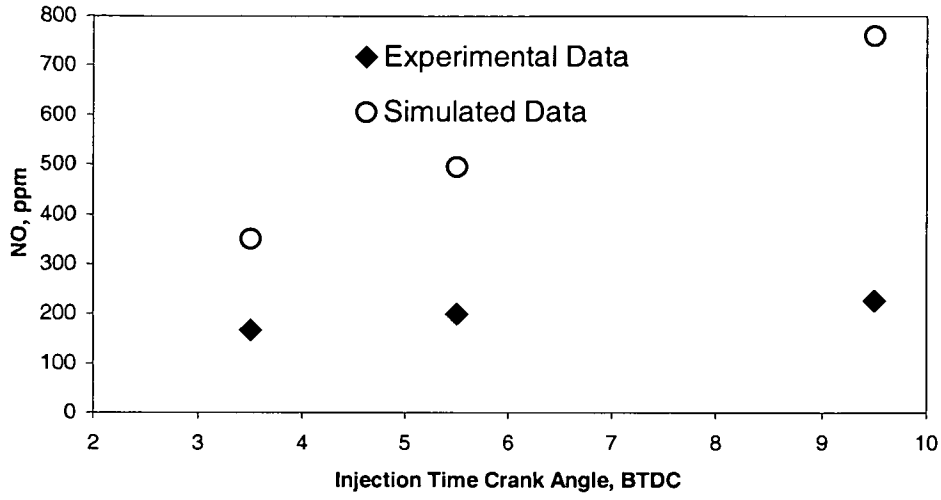

Figure 5.10: Comparison between the measured and the calculated NOx generated

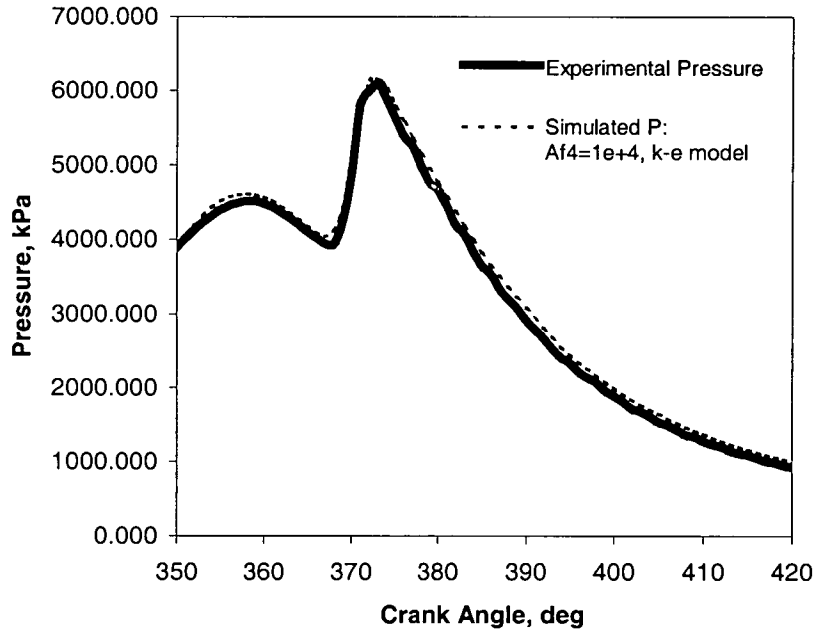

Fig 5.11: Pressure trace, experimental vs simulated for injection timing 5.5 degrees BTDC, 10 mg of fuel injected

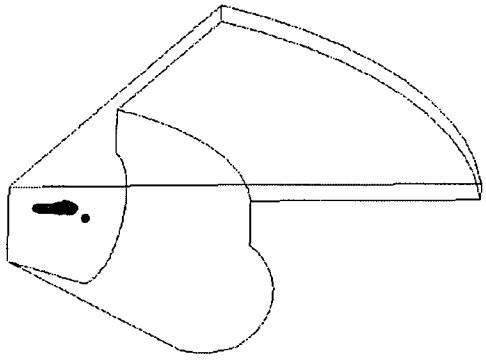

Fig 5. 12: Fuel parcel distribution, 5 degrees ATDC for Case B

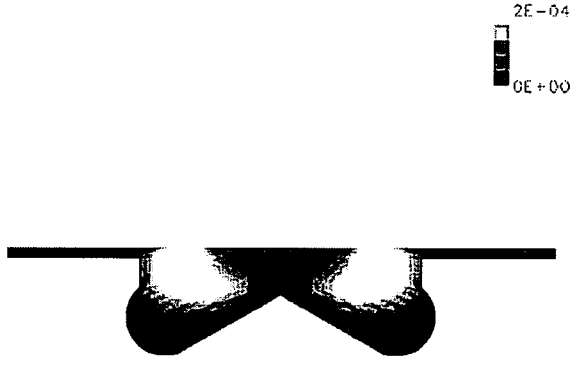

Fig 5. 13: Fuel vapor distribution at 5 degrees ATDC, Case B.

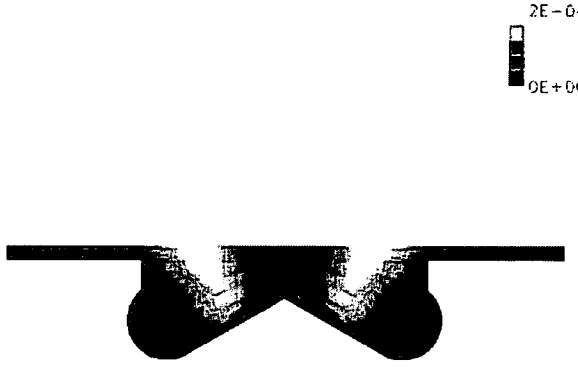

Fig 5. 14: Fuel vapor distribution at 20 degrees ATDC, Case B.

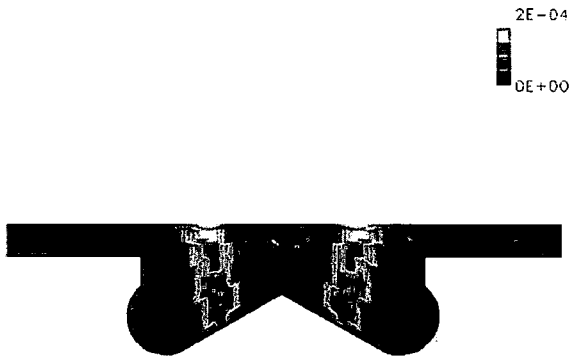

Fig 5. 15: Fuel vapor distribution at 30 degrees ATDC, Case B.

CHAPTER 6

CONCLUSIONS

6.1 General Conclusions

An integrated model for diesel ignition and combustion has been inserted into the software KIVA-3V2 and applied to the HSDI engine available at UIUC. The results show good levels of agreement between the computed and the measured data including ignition delay and, with a calibration factor, NOx emissions. Further work can be carried out to see if other parameters, such as soot generation and spray penetration can be matched. To model the ignition delay correctly, the low temperature chemistry of hydrocarbon kinetics i.e. the Shell model in this case is sufficient to predict the diesel spray ignition inside the high-speed diesel engine (HSDI).

The Shell model was applied to the HSDI and three different injection timings were tested. For all the injection timing tested, the overall pressure trace were well predicted with no changes in model constants. The NOx prediction however displays a different trend than expected, but previous researchers' results had even lower correlations.

Turbulence modeling was found to be essential in getting the combustion prediction right. The RNG k-e model is not applicable in this simulation as it causes too early ignition to take place. The standard k-e model was found to be a better model in this

situation. A possible explanation is the fact that the RNG k-e model causes the levels of turbulence predicted to be great, leading to faster evaporation of the spray that leads to more autoignition-related radical formation.

Although no comparisons were made with in-cylinder image data, good agreements with experimental data suggests that the spray model is able to capture the fuel distribution accurately. Therefore the predicted spray distribution can be accepted with some degree of certainty.

The most notable findings of this research would be:

1. The Shell model constants are still valid past the value of 1100K set as a limit by previous researchers. This might account for the discrepancy in NOx data, but that cannot be discerned as of yet.
2. The equation for the consumption of oxygen in the Shell model should not be limited to the steady-state equation defined by the originators of the Shell model but can be defined as a differential equation as shown in Chapter 3.

6.2 Future Work

As pointed out, although the model is able to predict the pressure trace well, there are many possible avenues for improvement. These are listed below.

i. The inclusion of crevice volume into the grid. This might account for the discrepancy in peak pressure. The small crevice volume becomes a significant percentage of the combustion chamber especially ATDC when combustion is due to happen.

ii. Improving the NOx prediction model is necessary to make the code applicable over a wide range of engines. The calibration factor might work for only this geometry and fail for others, but more extensive testing is required to verify this.

iii. Applying the model to other engine geometries is one good strategy to further verify the code. A different value of Shell model constants might be required to match the different geometries.

iv. Investigation into the failure of the laminar-turbulent model in predicting the combustion pressure should be done. With just the laminar model, the combustion proceeds as a totally premixed combustion phase that is not quite an accurate picture of what happens inside an HSDI.

v. Switching on the soot model will increase the utility of this code. Further improvements on this model will allow better approximation of engine emissions, a known problem with diesel engines.

vi. Heat release rates calculated numerically will be compared to the one obtained from experimental results.

With the recommended work, it is hoped that the code can be further improved upon making it very useful for future students in their engine studies.

LIST OF REFERENCES

1.Echols, L.S., Yust, V.E. and Bame, J.L., "A Review of Research on Abnormal Combustion Phenomena in Internal Combustion Engines", Proc. 5th World Petroleum Congress 1959, Section VI 159

2. Falk, K.G., "The Ignition Temperature of Hydrogen-Oxygen Mixtures", Journal of Am. Chem. Soc. 1906, Vol 28, pg 1517

3. Affleck, W.S., Fish, A., "Two-stage Ignition under Engine Conditions Parallels That at Low Pressures", 11th Int. Symposium on Combustion 1967, 1003 (The Combustion Institute, Pittsburgh)

4. Fish, A., "The Non-Thermal Oxidation of Neopentane", Combust. Flame 1969, Vol 2, pp 23-32

5. Martinengo, A., Oxidation Combustion Review 1967, Vol 2, pg 207

6. Voinov, A. N., Skorodelov, D.I., Sokolov, F. P., Kinetic Katalog 1964, Vol 5, pg 388

7. Fish, A., Haskell, W. W., Reed, I.A., "The Controlling Role Of Cool Flames In Two Stage Ignition", Combust. Flame 1969, Vol 13, pg 29

8. Affleck, W.S., Fish A., "Knock: Flame acceleration or spontaneous ignition?", Combust. Flame 1968, Vol 12, pg 243

9. Affleck, W.S., Thomas, A., "An Opposed Piston Rapid Compression Machine for Pre Flame Reaction Studies", Proc. Of the Institution of Mech. Engineers, 1968, Vol 183, Pt 1, No 19

10. Hirst, S.L., Kirsch, L.J., "The Application of a Hydrocarbon Autoignition Model in Simulation of Knock and other Engine Combustion Phenomena", in Combustion

Modeling in Reciprocating Engines (ed. C. Amann and J. Mattavi), Plenum Press, 1980

11. Halstead, M.P., Kirsch, L.J., Prothero, A., Quinn, C.P., "A Mathematical Model For Hydrocarbon Autoignition At High Pressures", Proc. R. Soc. Lond., A346, 1975
12. Halstead, M.P., Prothero, A., Quinn, C.P., Proc. Roya. Soc. London 1971, A322, pg377
13. Fish., A., Read, A., Affleck, W.S., Haskell, W.W., Proc. Roy. Soc. London 1969, A323, pg 261
14. Yang, C.H., Journal of Physical Chemistry 1969, Vol 73, pg 3407
15. Griffiths, J.F., Felton, P.G., Gray, P., 14th Symposium (int.) Combustion, Pittsburgh: The Combustion Institute, pg 453 1973
16. Halstead, M.P., Kirsch, L.J., Quinn, C.P., "The Autoignition of Hydrocarbon Fuels at High Temperatures and Pressure – Fitting of Mathematical Model", Combustion and Flame, 1977, Vol 30, pg 45-60
17. B. Natarajan, Bracco, F.V., "The Multidimensional Modeling of Auto-Ignition in Spark-Ignition Engines", Combustion and Flame, Vol57, 1984 pg179-197
18. Schapertons, H., and Lee, W., "Multidimensional Modeling of Knocking Combustion in SI Engines", SAE 850502
19 Pitsch, H., Peters, N., "Investigation of the Ignition Process of Sprays under Diesel Engine Conditions Using Reduced n-Heptane Chemistry", SAE 982464, 1998.
20. S.C. Kong, R. Reitz, "Multidimensional Modeling of Diesel Ignition and Combustion Using a Multistep Kinetics Model", Journal Eng. Gas Turbines and Power, October 1993, Vol 115, pg 781-789

21. S.C. Kong, Z. Han, Rolf Reitz, "The Development and Application of a Diesel Ignition and Combustion Model for Multidimensional Engine Simulation", SAE 950278

22. S.S. Sazhin, E.M. Sazhina, M.R. Heikal, C. Marooney, "The Shell Autoignition Model: A New Mathematical Formulation", Combustion and Flame, Vol 117 pg 529-540

23. A.A. Amsden, J.D. Ramshaw, P.J. O'Rourke, and J.K. Dukowicz, "KIVA: A Computer Program for Two- and three-dimensional Fluid Flows with Chemical Reactions and Fuel Sprays, "Los Alamos National Laboratory report LA-10245-MS (February 1985).

24. Amsden, A.A., J.D. Ramshaw, L.D. Cloutman, and P.J. O'Rourke, "Improvements and Extensions to the KIVA Computer Program, " Los Alamos National Laboratory report LA-10534-ms (October 1985).

24. A.A. Amsden, T.D. Butler, P.J. O'Rourke, and J.D. Ramshaw, "KIVA: A Comprehensive Model for 2D and 3D Engine Simulations," DAE Technical paper 8505

25. Amsden, A.A, O'Rourke, P.J., Butler, T.D., "KIVA-II, A Computer Program For Chemically Reactive Flows With Sprays", Los Alamos National Laboratory report LA-11560-MS (May 1989)

26. Amsden, A.A, KIVA-3: "A KIVA Program with Block-Structured Mesh for Complex Geometries", Los Alamos National Laboratory report LA-12503-MS (March 1993)

27. Amsden, A.A, "KIVA-3V: A Block-Structured KIVA Program for Engines with Vertical or Canted Valves", Los Alamos National Laboratory report LA-13313-MS (July 1997)

28. Amsden, A.A, "KIVA-3V2:Release 2, Improvements to KIVA-3V", Los Alamos National Laboratory report LA-UR-99-915 (May 1999)

29. Y. Zeng, C.F. Lee, "A Preferential Vaporization Model for Multicomponent Droplets and Sprays", accepted for publication in Atomization and Sprays, 2001

30. Schäpertons, H., "Simulation von Kloopfvorgangen mit einem zweidimensioalen mathematischen Modell", Dissertation TH Aachen 1984.

31. Hu, H., Keck, J., "Autoignition of Adiabatically Compressed Combustible Gas Mixtures", SAE Paper 872110, 1987

32. Heywood, J.B., Internal Combustion Engine Fundamentals, 1988 McGraw-Hill, pg 570-578

33. Bowman, C.T., "Kinetics of Pollutant Formation and Destruction in Combustion", Prog. Ebergy Combustion Sci., Vol 1, pp 33-45, 1975

34. Patterson, M.A., Kong, S.C., Hampson, G. J., Reitz, R.D., "Modelling the Effects of Fuel Injection Characteristics on Diesel Engine Soot and NOx Emissions", SAE Paper 940523, 1994.

APPENDIX A: INPUT FILES IN KIVA

As mentioned in the thesis, there are several input files to KIVA, namely:

A. IPREP: Defines the general shape of the computational domain that is to simulate actual model. Read by the mesh generator software K3PREP, part of KIVA's pre-processor software

B. ITAPE17: Mesh input file. Read by the executable. Defines the position of all vertices in the mesh and their connectivity.

C. ITAPE5: Operating parameter input file: Read by executable. Defines some geometric parameters of the mesh, but mainly contains information on the operating conditions to be simulated by the executable, for example the fuel introduction rate, species to be modeled and chemical equations

D. ITAPE7: Restart file. Read by executable, required if a run is to be restarted from a point where it stopped. Generated by executable as OTAPE8.

Files 1,2 and 3 are presented in this appendix as an example of the format and typical values used in the simulation. Refer to KIVA documentation for more information.

1. IPREP for Thornton RCM case

```
K3PREP/071202 Thornton RCM, 60-degree sector
  bore      3.81
  stroke   34.131
  squish  3.969
  thsect   60.0
 nblocks    2
   1   6   6  30   0   2   1   0
  1.0      1.0      0.0      0.0      1.0      1.0      0.0      0.0
  0.0      0.0      0.0      0.0      0.0      0.0      0.0      0.0
  3.3      3.3      3.3      3.3      3.3      3.3      3.3      3.3
  3.0      4.0      5.0      6.0      1.0      2.0
 -1.0     -1.0     -1.0     -1.0      0.0     -1.0
   2   7   6  30   0   2   1   0
  1.90     1.90     1.0      1.0      1.90     1.90     1.0      1.0
  0.0      0.0      0.0      0.0      0.0      0.0      0.0      0.0
  3.3      3.3      3.3      3.3      3.3      3.3      3.3      3.3
  4.0      2.0      5.0      6.0      1.0      2.0
 -1.0     -1.0     -1.0     -1.0      0.0     -1.0
  ncopy    0
  tiltflag    0
  pentflag    0
 wedgeflag    0
 translate    0
   nlocxy     0
   reshape    0
 npentxy      0
 nvguide      0
 nvalvport    0
 nrunner      0
 nsiamese     0
 nround       0
    npatch    1
   2   1   1   1   1   1
   nrelaxb    0
  nprovtop    0
  nprovfce    0
 nzcylwall    0
     tilt     0
 ndish        0
 nscallop     0
 xoffset   0.0
 yoffset   0.0
 write17   1.0
plotmesh   1.0
  xband    0.1
  yband    0.1
  zband    0.1
 nxplots    0
 nyplots    1
  0.0
 nzplots    0
  nvhide    0
```

2. ITAPE5 for Thornton RCM case

```
MS Thesis: RCM
  irest      0
 nohydro     0
  lwall      1
  lpr        0
  irez       2
  ncfilm 9999
  nctap8  100
  nclast99999
  ncmon      1
 ncaspec     0
  gmv        0.0
  cafilm    9.99e+9
  cafin   1182.0
  angmom     0.0
  pgssw      0.0
  dti    1.00000e-5
  dtmxca     1.0
  dtmax 1.00000e-4
  tlimd      1.0
  twfilm    1.00e-2
  twfin     0.176
  fchsp      0.25
  bore       3.81
  stroke    34.131
  squish     3.969
  rpm       2900.0
  atdc     180.0
  datdct     0.0
  revrep     2.0
  conrod    27.0
  swirl      0.0
  swipro     3.11
  thsect    60.0
  sector     1.0
  deact      0.0
  epsy       1.0e-3
  epsv       1.0e-3
  epsp       1.0e-4
  epst       1.0e-3
  epsk       1.0e-3
  epse       1.0e-3
  gx         0.0
  gy         0.0
  gz         0.0
  tcylwl   373.00
  thead    373.00
  tpistn   373.00
  pardon     0.0
  a0         0.0
  b0         1.0
  artvis     0.0
  ecnsrv     0.0
  adia       0.0
```

```
 anu0       0.0
 visrat-.66666667
 tcut    1100.0
 tcute   1200.0
 epschm     0.02
 omgchm     1.0
 turbsw     2.0
 sgsl       4.0
trbchem     0.0
 capa      18.0
pmplict     2.0
lospeed     0.0
 airmu1   1.457e-5
 airmu2   110.0
 airla1   252.0
 airla2   200.0
 prl        0.74
 rpr        1.11
 rsc        1.11
 xignit     1.0e+4
 t1ign     -1.0
 tdign     -1.0
 ca1ign   9.e99
 cadign    0.0
 xignl1    +1.600
 xignr1    +2.000
 yignf1    -0.200
 yignd1    +0.200
 zignb1    7.0000
 zignt1    7.6000
 xignl2     0.0
 xignr2     0.0
 yignf2     0.0
 yignd2     0.0
 zignb2     0.0
 zignt2     0.0
 kwikeq     0
 numnoz     1
 numinj     1
 numvel     1
 t1inj     -1.0
 tdinj     -1.0
 ca1inj 9900.0
 cadinj    8.4
 tspmas    0.00534
 tnparc       0.0
 pulse      2.0
injdist     0
 kolide     1
 tpi      273.15
 turb       1.0
breakup     1.0
 evapp      0.0
 drnoz    0.2485
 dznoz    7.6725
 dthnoz     30.0
 tiltxy     30.0
```

```
  tiltxz    75.0
  cone      10.0
  dcone     10.0
  anoz      7.248e-4
  smr       62.0e-4
  amp0       0.0
    19650.0
  nsp       19    4
  ic8h18     1.00000
  ic5h12     0.00000
   c7h16     0.00000
   c6h14     0.00000
      o2    mw2      32.000  htf2      0.0
      n2    mw3      28.016  htf3      0.0
     co2    mw4      44.011  htf4    -93.965
     h2o    mw5      18.016  htf5    -57.103
       h    mw6       1.008  htf6     51.631
      h2    mw7       2.016  htf7      0.0
       o    mw8      16.000  htf8     58.989
       n    mw9      14.008  htf9    112.520
      oh    mw10     17.008  htf10     9.289
      co    mw11     28.011  htf11   -27.200
      no    mw12     30.008  htf12    21.456
      r*    mw13     73.116  htf13     0.0
      b     mw14    146.232  htf14     0.0
      q     mw15    146.232  htf15     0.0
      p     mw16     25.204  htf16     0.0
model option
0  0  0  0
stoifuel    2.0
  stoio2   25.0
  nreg      1
 presi,     9.8040e+5
 tempi,     373.0
 tkei,      0.10
 scli,      0.0
 er,        0.0
 mfracfu,   0.05620
 mfracfu,   0.00000
 mfracfu,   0.00000
 mfracfu,   0.00000
 mfraco2,   0.20805
 mfracn2,   0.72175
 mfracco2,  0.00933
 mfrach2o,  0.00467
 mfrach,    0.0
 mfrach2,   0.0
 mfraco,    0.0
 mfracn,    0.0
 mfracoh,   0.0
 mfracco,   0.0
 mfracno,   0.0
 mfracr*,   0.0
 mfracb,    0.0
 mfracq,    0.0
 mfracp,    0.0
  nrk      15
```

```
cf1   4.6000e11 ef1   1.5078e+4 zf1       0.0
cb1      0.0    eb1      0.0    zb1       0.0
am1        2         0         0         0        25         0         0         0
           0         0         0         0         0         0         0         0
           0         0         0         0
bm1        0         0         0         0         0         0        16        18
           0         0         0         0         0         0         0         0
           0         0         0         0
ae1    0.250     0.000     0.000     0.000     1.500     0.000     0.000     0.000
       0.000     0.000     0.000     0.000     0.000     0.000     0.000     0.000
       0.000     0.000     0.000     0.000
be1    0.000     0.000     0.000     0.000     0.000     0.000     0.000     0.000
       0.000     0.000     0.000     0.000     0.000     0.000     0.000     0.000
       0.000     0.000     0.000     0.000
cf2   1.1100e11 ef1   1.5078e+4 zf1       0.0
cb2      0.0    eb1      0.0    zb1       0.0
am2        0         1         0         0         8         0         0         0
           0         0         0         0         0         0         0         0
           0         0         0         0
bm2        0         0         0         0         0         0         5         0
           6         0         0         0         0         0         0         0
           0         0         0         0
ae2    0.000     0.250     0.000     0.000     1.500     0.000     0.000     0.000
       0.000     0.000     0.000     0.000     0.000     0.000     0.000     0.000
       0.000     0.000     0.000     0.000
be2    0.000     0.000     0.000     0.000     0.000     0.000     0.000     0.000
       0.000     0.000     0.000     0.000     0.000     0.000     0.000     0.000
       0.000     0.000     0.000     0.000
cf3   9.9000e10 ef1   1.5078e+4 zf1       0.0
cb3      0.0    eb1      0.0    zb1       0.0
am3        0         2         0         0        19         0         0         0
           0         0         0         0         0         0         0         0
           0         0         0         0
bm3        0         0         0         0         0         0        12         0
          14         0         0         0         0         0         0         0
           0         0         0         0
ae3    0.000     0.250     0.000     0.000     1.500     0.000     0.000     0.000
       0.000     0.000     0.000     0.000     0.000     0.000     0.000     0.000
       0.000     0.000     0.000     0.000
be3    0.000     0.000     0.000     0.000     0.000     0.000     0.000     0.000
       0.000     0.000     0.000     0.000     0.000     0.000     0.000     0.000
       0.000     0.000     0.000     0.000
cf4   8.0000e10 ef1   1.5078e+4 zf1       0.0
cb4      0.0    eb1      0.0    zb1       0.0
am4        0         0         2         0        25         0         0         0
           0         0         0         0         0         0         0         0
           0         0         0         0
bm4        0         0         0         0         0         0         6         0
          18         0         0         0         0         0         0         0
           0         0         0         0
ae4    0.000     0.000     0.250     0.000     0.150     0.000     0.000     0.000
       0.000     0.000     0.000     0.000     0.000     0.000     0.000     0.000
       0.000     0.000     0.000     0.000
be4    0.000     0.000     0.000     0.000     0.000     0.000     0.000     0.000
       1.000     0.000     0.000     0.000     0.000     0.000     1.000     0.000
       0.000     0.000     0.000     0.000
cf5   1.5587e14 ef2   6.7627e+4 zf2       0.0
```

```
cb5   7.5000e12 eb2       0.0     zb2       0.0
am5         0        0        0        0        1        2        0        0
            0        0        0        0        0        0        0        0
            0        0        0        0
bm5         0        0        0        0        0        0        0        0
            0        0        0        2        0        0        2        0
            0        0        0        0
ae5     0.000    0.000    0.000    0.000    0.500    1.000    0.000    0.000
        0.000    0.000    0.000    0.000    0.000    0.000    0.000    0.000
        0.000    0.000    0.000    0.000
be5     0.000    0.000    0.000    0.000    0.000    0.000    0.000    0.000
        0.000    0.000    0.000    1.000    0.000    0.000    1.000    0.000
        0.000    0.000    0.000    0.000
cf6   2.6484e10 ef3    5.9418e+4 zf3       1.0
cb6   1.6000e+9 eb3    1.9678e+4 zb3       1.0
am6         0        0        0        0        2        1        0        0
            0        0        0        0        0        0        0        0
            0        0        0        0
bm6         0        0        0        0        0        0        0        0
            0        0        2        0        0        0        2        0
            0        0        0        0
ae6     0.000    0.000    0.000    0.000    1.000    0.500    0.000    0.000
        0.000    0.000    0.000    0.000    0.000    0.000    0.000    0.000
        0.000    0.000    0.000    0.000
be6     0.000    0.000    0.000    0.000    0.000    0.000    0.000    0.000
        0.000    0.000    1.000    0.000    0.000    0.000    1.000    0.000
        0.000    0.000    0.000    0.000
cf7   2.1230e14 ef4    5.7020e+4 zf4       0.0
cb7       0.0     eb4       0.0     zb4       0.0
am7         0        0        0        0        0        1        0        0
            0        0        0        0        2        0        0        0
            0        0        0        0
bm7         0        0        0        0        0        0        0        0
            2        0        0        0        0        0        2        0
            0        0        0        0
ae7     0.000    0.000    0.000    0.000    0.000    0.500    0.000    0.000
        0.000    0.000    0.000    0.000    1.000    0.000    0.000    0.000
        0.000    0.000    0.000    0.000
be7     0.000    0.000    0.000    0.000    0.000    0.000    0.000    0.000
        1.000    0.000    0.000    0.000    0.000    0.000    1.000    0.000
        0.000    0.000    0.000    0.000
cf8   1.200e12   ef8    1.7591e+4 zf8       0.0
cb8       0.0     eb8       0.0     zb8       0.0
am8         1        0        0        0        1        0        0        0
            0        0        0        0        0        0        0        0
            0        0        0        0
bm8         0        0        0        0        0        0        0        0
            0        0        0        0        0        0        0        2
            0        0        0        0
ae8     0.000    0.000    0.000    0.000    0.000    0.000    0.000    0.000
        0.000    0.000    0.000    0.000    0.000    0.000    0.000    0.000
        0.000    0.000    0.000    0.000
be8     0.000    0.000    0.000    0.000    0.000    0.000    0.000    0.000
        0.000    0.000    0.000    0.000    0.000    0.000    0.000    0.000
        0.000    0.000    0.000    0.000
cf9   0.500e10   ef9    0.0000e+0 zf9       0.0
cb9       0.0     eb9       0.0     zb9       0.0
```

```
am9         0       0       0       0       0       0       0       0
            0       0       0       0       0       0       0       1
            0       0       0       0
bm9         0       0       0       0       0       0       0       0
            0       0       0       0       0       0       0       1
            0       0       0       0
ae9     0.000   0.000   0.000   0.000   0.000   0.000   0.000   0.000
        0.000   0.000   0.000   0.000   0.000   0.000   0.000   0.000
        0.000   0.000   0.000   0.000
be9     0.000   0.000   0.000   0.000   0.000   0.000   0.000   0.000
        0.000   0.000   0.000   0.000   0.000   0.000   0.000   0.000
        0.000   0.000   0.000   0.000
cf10  0.500e10  ef10  0.0000e+0 zf10      0.0
cb10     0.0    eb10     0.0    zb10      0.0
am10        0       0       0       0       0       0       0       0
            0       0       0       0       0       0       0       0
            0       0       0       0
bm10        0       0       0       0       0       0       0       0
            0       0       0       0       0       0       0       0
            0       0       0       0
ae10    0.000   0.000   0.000   0.000   0.000   0.000   0.000   0.000
        0.000   0.000   0.000   0.000   0.000   0.000   0.000   0.000
        0.000   0.000   0.000   0.000
be10    0.000   0.000   0.000   0.000   0.000   0.000   0.000   0.000
        0.000   0.000   0.000   0.000   0.000   0.000   0.000   0.000
        0.000   0.000   0.000   0.000
cf11  1.700e+4  ef11  0.0000e+0 zf11      0.0
cb11     0.0    eb11     0.0    zb11      0.0
am11        0       0       0       0       0       0       0       0
            0       0       0       0       0       0       0       0
            0       0       0       0
bm11        0       0       0       0       0       0       0       0
            0       0       0       0       0       0       0       0
            0       0       0       0
ae11    0.000   0.000   0.000   0.000   0.000   0.000   0.000   0.000
        0.000   0.000   0.000   0.000   0.000   0.000   0.000   0.000
        0.000   0.000   0.000   0.000
be11    0.000   0.000   0.000   0.000   0.000   0.000   0.000   0.000
        0.000   0.000   0.000   0.000   0.000   0.000   0.000   0.000
        0.000   0.000   0.000   0.000
cf12  0.500e10  ef12  0.0000e+0 zf12      0.0
cb12     0.0    eb12     0.0    zb12      0.0
am12        0       0       0       0       0       0       0       0
            0       0       0       0       0       0       0       1
            0       1       0       0
bm12        0       0       0       0       0       0       0       0
            0       0       0       0       0       0       0       1
            1       0       0       0
ae12    0.000   0.000   0.000   0.000   0.000   0.000   0.000   0.000
        0.000   0.000   0.000   0.000   0.000   0.000   0.000   0.000
        0.000   0.000   0.000   0.000
be12    0.000   0.000   0.000   0.000   0.000   0.000   0.000   0.000
        0.000   0.000   0.000   0.000   0.000   0.000   0.000   0.000
        0.000   0.000   0.000   0.000
cf13  4.400e17  ef13  2.2617e+4 zf13      0.0
cb13     0.0    eb13     0.0    zb13      0.0
am13        0       0       0       0       0       0       0       0
```

```
            0       0       0       0       0       0       0       0
            1       0       0       0
 bm13       0       0       0       0       0       0       0       0
            0       0       0       0       0       0       0       2
            0       0       0       0
 ae13   0.000   0.000   0.000   0.000   0.000   0.000   0.000   0.000
        0.000   0.000   0.000   0.000   0.000   0.000   0.000   0.000
        0.000   0.000   0.000   0.000
 be13   0.000   0.000   0.000   0.000   0.000   0.000   0.000   0.000
        0.000   0.000   0.000   0.000   0.000   0.000   0.000   0.000
        0.000   0.000   0.000   0.000
 cf14  1.000e12  ef14  0.0000e+0 zf14     0.0
 cb14     0.0    eb14     0.0    zb14     0.0
 am14       0       0       0       0       0       0       0       0
            0       0       0       0       0       0       0       1
            0       0       0       0
 bm14       0       0       0       0       0       4       0       0
            0       0       0       0       0       0       0       0
            0       0       0       0
 ae14   0.000   0.000   0.000   0.000   0.000   0.000   0.000   0.000
        0.000   0.000   0.000   0.000   0.000   0.000   0.000   0.000
        0.000   0.000   0.000   0.000
 be14   0.000   0.000   0.000   0.000   0.000   0.000   0.000   0.000
        0.000   0.000   0.000   0.000   0.000   0.000   0.000   0.000
        0.000   0.000   0.000   0.000
 cf15  3.000e11  ef15  0.0000e+0 zf15     0.0
 cb15     0.0    eb15     0.0    zb15     0.0
 am15       0       0       0       0       0       0       0       0
            0       0       0       0       0       0       0       2
            0       0       0       0
 bm15       0       0       0       0       0       8       0       0
            0       0       0       0       0       0       0       0
            0       0       0       0
 ae15   0.000   0.000   0.000   0.000   0.000   0.000   0.000   0.000
        0.000   0.000   0.000   0.000   0.000   0.000   0.000   0.000
        0.000   0.000   0.000   0.000
 be15   0.000   0.000   0.000   0.000   0.000   0.000   0.000   0.000
        0.000   0.000   0.000   0.000   0.000   0.000   0.000   0.000
        0.000   0.000   0.000   0.000
  nre       6
 as1   0.990207  bs1   -51.7916  cs1   0.993074  ds1  -0.343428  es1
0.0111668
 an1        0       0       0       0       0       0       0       0
            0       1       0       0       0       0       0       0
            0       0       0       0
 bn1        0       0       0       0       0       0       0       0
            2       0       0       0       0       0       0       0
            0       0       0       0
 as2   0.431310  bs2   -59.6554  cs2   3.503350  ds2  -0.340016  es2
0.0158715
 an2        0       0       0       0       1       0       0       0
            0       0       0       0       0       0       0       0
            0       0       0       0
 bn2        0       0       0       0       0       0       0       0
            0       0       2       0       0       0       0       0
            0       0       0       0
```

```
 as3    0.794709  bs3   -113.2080  cs3    3.168370  ds3   -0.443814  es3
0.0269699
 an3          0         0         0         0         0         1         0         0
              0         0         0         0         0         0         0         0
              0         0         0         0
 bn3          0         0         0         0         0         0         0         0
              0         0         0         2         0         0         0         0
              0         0         0         0
 as4   -0.652939  bs4     -9.8232  cs4    3.930330  ds4    0.163490  es4   -
0.0142865
 an4          0         0         0         0         1         0         0         0
              0         1         0         0         0         0         0         0
              0         0         0         0
 bn4          0         0         0         0         0         0         0         0
              0         0         0         0         2         0         0         0
              0         0         0         0
 as5    1.158882  bs5    -76.8472  cs5    8.532155  ds5   -0.868320  es5
0.0463471
 an5          0         0         0         0         1         0         0         2
              0         0         0         0         0         0         0         0
              0         0         0         0
 bn5          0         0         0         0         0         0         0         0
              0         0         0         0         4         0         0         0
              0         0         0         0
 as6    0.980875  bs6     68.4453  cs6   -10.5938   ds6    0.574260  es6   -
0.0414570
 an6          0         0         0         0         1         0         0         0
              0         0         0         0         0         2         0         0
              0         0         0
 bn6          0         0         0         0         0         0         2         0
              0         0         0         0         0         0         0         0
              0         0         0
 nvalves      0
  isoot       0
```

3. ITAPE5 for HSDI case

```
MS Thesis: HSDI Diesel Engine with Shell autoignition model
  irest      2
 nohydro     0
  lwall      1
  lpr        0
  irez       2
  ncfilm  9999
  nctap8    50
  nclast  9999
  ncmon      1
 ncaspec     0
  gmv        0.0
  cafilm    9.99e+9
  cafin    420.0
  angmom     0.0
  pgssw      0.0
  dti    1.00000e-5
  dtmxca     1.0
  dtmax 1.00000e-4
  tlimd      1.0
  twfilm    9.99e+9
  twfin     9.99e+9
  fchsp      0.25
  bore       7.00
  stroke     7.80
  squish     0.1153
  rpm       2000.0
  atdc     180.0
  datdct     0.0
  revrep     2.0
  conrod    13.26
  swirl      4.0
  swipro     3.11
  thsect    60.0
  sector     1.0
  deact      0.0
  epsy       1.0e-3
  epsv       1.0e-3
  epsp       1.0e-4
  epst       1.0e-3
  epsk       1.0e-3
  epse       1.0e-3
  gx         0.0
  gy         0.0
  gz         0.0
  tcylwl   330.00
  thead    330.00
  tpistn   480.00
  pardon     0.0
  a0         0.0
  b0         1.0
  artvis     0.0
  ecnsrv     0.0
  adia       0.0
```

```
 anu0       0.0
 visrat~.66666667
 tcut    1150.0
 tcute   1200.0
 epschm     0.02
 omgchm     1.0
 turbsw     2.0
 sgsl       4.0
trbchem     0.0
 capa       1.0
pmplict     2.0
lospeed     0.0
 airmu1   1.457e-5
 airmu2   110.0
 airla1   252.0
 airla2   200.0
 prl        0.74
 rpr        1.11
 rsc        1.11
 xignit     1.0e+4
 tlign     -1.0
 tdign     -1.0
 calign   9.e99
 cadign    0.0
 xignl1    +1.600
 xignr1    +2.000
 yignf1    -0.200
 yignd1    +0.200
 zignb1    7.0000
 zignt1    7.6000
 xignl2     0.0
 xignr2     0.0
 yignf2     0.0
 yignd2     0.0
 zignb2     0.0
 zignt2     0.0
 kwikeq     0
 numnoz     1
 numinj     1
 numvel     1
 tlinj     -1.0
 tdinj     -1.0
 calinj   354.5
 cadinj   10.0
 tspmas    0.00534
 tnparc    1000.0
 pulse      2.0
injdist     0
 kolide     1
 tpi      353.15
 turb       1.0
breakup     1.0
 evapp      1.0
 drnoz    0.2485
 dznoz    7.6725
 dthnoz     30.0
 tiltxy     30.0
```

```
  tiltxz    75.0
  cone      10.0
  dcone     10.0
  anoz      7.248e-4
  smr       62.0e-4
  amp0       0.0
    19650.0
  nsp       18     4
  c14h30     1.00000
  ic5h12     0.00000
   c6h14     0.00000
  ic8h18     0.00000
      o2    mw2      32.000  htf2      0.0
      n2    mw3      28.016  htf3      0.0
     co2    mw4      44.011  htf4    -93.965
     h2o    mw5      18.016  htf5    -57.103
       h    mw6       1.008  htf6     51.631
      h2    mw7       2.016  htf7      0.0
       o    mw8      16.000  htf8     58.989
       n    mw9      14.008  htf9    112.520
      oh    mw10     17.008  htf10     9.289
      co    mw11     28.011  htf11   -27.200
      no    mw12     30.008  htf12    21.456
      r*    mw13    115.197  htf13     0.000
      b     mw14    230.394  htf14     0.000
      q     mw15    230.394  htf15     0.000
model option
1  1  1  1
stoifuel     2.0
  stoio2    43.0
  nreg       1
 presi,      1.0000e+6
 tempi,      415.0
 tkei,       0.10
 scli,       0.0
 er,         0.0
 mfracfu,    0.00000
 mfracfu,    0.00000
 mfracfu,    0.00000
 mfracfu,    0.00000
 mfraco2,    0.18705
 mfracn2,    0.78186
 mfracco2,   0.01451
 mfrach2o,   0.01255
 mfrach,     0.0
 mfrach2,    0.00001
 mfraco,     0.00001
 mfracn,     0.0
 mfracoh,    0.0
 mfracco,    0.0
 mfracno,    0.0
 mfracr*,    0.0
 mfracb,     0.0
 mfracq,     0.0
  nrk       15
 cf1    2.2000e11 ef1    1.5078e+4 zf1       0.0
 cb1       0.0    eb1       0.0    zb1       0.0
```

```
am1         2         0         0         0        43         0         0         0
            0         0         0         0         0         0         0         0
            0         0         0
bm1         0         0         0         0         0         0        28        30
            0         0         0         0         0         0         0         0
            0         0         0
ae1     0.250     0.000     0.000     0.000     1.500     0.000     0.000     0.000
        0.000     0.000     0.000     0.000     0.000     0.000     0.000     0.000
        0.000     0.000     0.000
be1     0.000     0.000     0.000     0.000     0.000     0.000     0.000     0.000
        0.000     0.000     0.000     0.000     0.000     0.000     0.000     0.000
        0.000     0.000     0.000
cf2   1.1100e11 ef1     1.5078e+4 zf1       0.0
cb2       0.0     eb1       0.0     zb1       0.0
am2         0         1         0         0         8         0         0         0
            0         0         0         0         0         0         0         0
            0         0         0
bm2         0         0         0         0         0         0         5         0
            6         0         0         0         0         0         0         0
            0         0         0
ae2     0.000     0.250     0.000     0.000     1.500     0.000     0.000     0.000
        0.000     0.000     0.000     0.000     0.000     0.000     0.000     0.000
        0.000     0.000     0.000
be2     0.000     0.000     0.000     0.000     0.000     0.000     0.000     0.000
        0.000     0.000     0.000     0.000     0.000     0.000     0.000     0.000
        0.000     0.000     0.000
cf3   9.9000e10 ef1     1.5078e+4 zf1       0.0
cb3       0.0     eb1       0.0     zb1       0.0
am3         0         2         0         0        19         0         0         0
            0         0         0         0         0         0         0         0
            0         0         0
bm3         0         0         0         0         0         0        12         0
           14         0         0         0         0         0         0         0
            0         0         0
ae3     0.000     0.250     0.000     0.000     1.500     0.000     0.000     0.000
        0.000     0.000     0.000     0.000     0.000     0.000     0.000     0.000
        0.000     0.000     0.000
be3     0.000     0.000     0.000     0.000     0.000     0.000     0.000     0.000
        0.000     0.000     0.000     0.000     0.000     0.000     0.000     0.000
        0.000     0.000     0.000
cf4   8.0000e10 ef1     1.5078e+4 zf1       0.0
cb4       0.0     eb1       0.0     zb1       0.0
am4         0         0         2         0        25         0         0         0
            0         0         0         0         0         0         0         0
            0         0         0
bm4         0         0         0         0         0         0         6         0
           18         0         0         0         0         0         0         0
            0         0         0
ae4     0.000     0.000     0.250     0.000     0.150     0.000     0.000     0.000
        0.000     0.000     0.000     0.000     0.000     0.000     0.000     0.000
        0.000     0.000     0.000
be4     0.000     0.000     0.000     0.000     0.000     0.000     0.000     0.000
        1.000     0.000     0.000     0.000     0.000     0.000     1.000     0.000
        0.000     0.000     0.000
cf5   1.5587e14 ef2     6.7627e+4 zf2       0.0
cb5   7.5000e12 eb2       0.0     zb2       0.0
am5         0         0         0         0         1         2         0         0
```

```
          0       0       0       0       0       0       0       0
          0       0       0
bm5       0       0       0       0       0       0       0       0
          0       0       0       2       0       0       2       0
          0       0       0
ae5   0.000   0.000   0.000   0.000   0.500   1.000   0.000   0.000
      0.000   0.000   0.000   0.000   0.000   0.000   0.000   0.000
      0.000   0.000   0.000
be5   0.000   0.000   0.000   0.000   0.000   0.000   0.000   0.000
      0.000   0.000   0.000   1.000   0.000   0.000   1.000   0.000
      0.000   0.000   0.000
cf6   2.6484e10 ef3   5.9418e+4 zf3       1.0
cb6   1.6000e+9 eb3   1.9678e+4 zb3       1.0
am6       0       0       0       0       2       1       0       0
          0       0       0       0       0       0       0       0
          0       0       0
bm6       0       0       0       0       0       0       0       0
          0       0       2       0       0       0       2       0
          0       0       0
ae6   0.000   0.000   0.000   0.000   1.000   0.500   0.000   0.000
      0.000   0.000   0.000   0.000   0.000   0.000   0.000   0.000
      0.000   0.000   0.000
be6   0.000   0.000   0.000   0.000   0.000   0.000   0.000   0.000
      0.000   0.000   1.000   0.000   0.000   0.000   1.000   0.000
      0.000   0.000   0.000
cf7   2.1230e14 ef4   5.7020e+4 zf4       0.0
cb7      0.0    eb4      0.0    zb4       0.0
am7       0       0       0       0       0       1       0       0
          0       0       0       0       2       0       0       0
          0       0       0
bm7       0       0       0       0       0       0       0       0
          2       0       0       0       0       0       2       0
          0       0       0
ae7   0.000   0.000   0.000   0.000   0.000   0.500   0.000   0.000
      0.000   0.000   0.000   0.000   1.000   0.000   0.000   0.000
      0.000   0.000   0.000
be7   0.000   0.000   0.000   0.000   0.000   0.000   0.000   0.000
      1.000   0.000   0.000   0.000   0.000   0.000   1.000   0.000
      0.000   0.000   0.000
cf8   1.200e12  ef8   1.7591e+4 zf8       0.0
cb8      0.0    eb8      0.0    zb8       0.0
am8       1       0       0       0       1       0       0       0
          0       0       0       0       0       0       0       0
          0       0       0
bm8       0       0       0       0       0       0       0       0
          0       0       0       0       0       0       0       2
          0       0       0
ae8   0.000   0.000   0.000   0.000   0.000   0.000   0.000   0.000
      0.000   0.000   0.000   0.000   0.000   0.000   0.000   0.000
      0.000   0.000   0.000
be8   0.000   0.000   0.000   0.000   0.000   0.000   0.000   0.000
      0.000   0.000   0.000   0.000   0.000   0.000   0.000   0.000
      0.000   0.000   0.000
cf9   0.500e10  ef9   0.0000e+0 zf9       0.0
cb9      0.0    eb9      0.0    zb9       0.0
am9       0       0       0       0       0       0       0       0
          0       0       0       0       0       0       0       1
```

```
          0       0       0
bm9       0       0       0       0       0       0       0       0
          0       0       0       0       0       0       0       1
          0       0       0
ae9   0.000   0.000   0.000   0.000   0.000   0.000   0.000   0.000
      0.000   0.000   0.000   0.000   0.000   0.000   0.000   0.000
      0.000   0.000   0.000
be9   0.000   0.000   0.000   0.000   0.000   0.000   0.000   0.000
      0.000   0.000   0.000   0.000   0.000   0.000   0.000   0.000
      0.000   0.000   0.000
cf10  0.500e10  ef10  0.0000e+0 zf10     0.0
cb10     0.0    eb10     0.0    zb10     0.0
am10      0       0       0       0       0       0       0       0
          0       0       0       0       0       0       0       1
          0       0       0
bm10      0       0       0       0       0       0       0       0
          0       0       0       0       0       0       0       1
          1       0       0
ae10  0.000   0.000   0.000   0.000   0.000   0.000   0.000   0.000
      0.000   0.000   0.000   0.000   0.000   0.000   0.000   0.000
      0.000   0.000   0.000
be10  0.000   0.000   0.000   0.000   0.000   0.000   0.000   0.000
      0.000   0.000   0.000   0.000   0.000   0.000   0.000   0.000
      0.000   0.000   0.000
cf11  1.700e+4  ef11  0.0000e+0 zf11     0.0
cb11     0.0    eb11     0.0    zb11     0.0
am11      0       0       0       0       0       0       0       0
          0       0       0       0       0       0       0       1
          0       0       0
bm11      0       0       0       0       0       0       0       0
          0       0       0       0       0       0       0       1
          0       1       0
ae11  0.000   0.000   0.000   0.000   0.000   0.000   0.000   0.000
      0.000   0.000   0.000   0.000   0.000   0.000   0.000   0.000
      0.000   0.000   0.000
be11  0.000   0.000   0.000   0.000   0.000   0.000   0.000   0.000
      0.000   0.000   0.000   0.000   0.000   0.000   0.000   0.000
      0.000   0.000   0.000
cf12  0.500e10  ef12  0.0000e+0 zf12     0.0
cb12     0.0    eb12     0.0    zb12     0.0
am12      0       0       0       0       0       0       0       0
          0       0       0       0       0       0       0       1
          0       1       0
bm12      0       0       0       0       0       0       0       0
          0       0       0       0       0       0       0       1
          1       0       0
ae12  0.000   0.000   0.000   0.000   0.000   0.000   0.000   0.000
      0.000   0.000   0.000   0.000   0.000   0.000   0.000   0.000
      0.000   0.000   0.000
be12  0.000   0.000   0.000   0.000   0.000   0.000   0.000   0.000
      0.000   0.000   0.000   0.000   0.000   0.000   0.000   0.000
      0.000   0.000   0.000
cf13  4.400e17  ef13  2.2617e+4 zf13     0.0
cb13     0.0    eb13     0.0    zb13     0.0
am13      0       0       0       0       0       0       0       0
          0       0       0       0       0       0       0       0
          1       0       0
```

```
bm13        0        0        0        0        0        0        0        0
            0        0        0        0        0        0        0        2
            0        0        0
ae13    0.000    0.000    0.000    0.000    0.000    0.000    0.000    0.000
        0.000    0.000    0.000    0.000    0.000    0.000    0.000    0.000
        0.000    0.000    0.000
be13    0.000    0.000    0.000    0.000    0.000    0.000    0.000    0.000
        0.000    0.000    0.000    0.000    0.000    0.000    0.000    0.000
        0.000    0.000    0.000
cf14   1.000e12   ef14   0.0000e+0 zf14      0.0
cb14      0.0     eb14      0.0     zb14      0.0
am14        0        0        0        0        0        0        0        0
            0        0        0        0        0        0        0        1
            0        0        0
bm14        0        0        0        0        0        4        0        0
            0        0        0        0        0        0        0        0
            0        0        0
ae14    0.000    0.000    0.000    0.000    0.000    0.000    0.000    0.000
        0.000    0.000    0.000    0.000    0.000    0.000    0.000    0.000
        0.000    0.000    0.000
be14    0.000    0.000    0.000    0.000    0.000    0.000    0.000    0.000
        0.000    0.000    0.000    0.000    0.000    0.000    0.000    0.000
        0.000    0.000    0.000
cf15   3.000e11   ef15   0.0000e+0 zf15      0.0
cb15      0.0     eb15      0.0     zb15      0.0
am15        0        0        0        0        0        0        0        0
            0        0        0        0        0        0        0        2
            0        0        0
bm15        0        0        0        0        0        8        0        0
            0        0        0        0        0        0        0        0
            0        0        0
ae15    0.000    0.000    0.000    0.000    0.000    0.000    0.000    0.000
        0.000    0.000    0.000    0.000    0.000    0.000    0.000    0.000
        0.000    0.000    0.000
be15    0.000    0.000    0.000    0.000    0.000    0.000    0.000    0.000
        0.000    0.000    0.000    0.000    0.000    0.000    0.000    0.000
        0.000    0.000    0.000
 nre        6
as1    0.990207  bs1    -51.7916  cs1    0.993074  ds1   -0.343428  es1
0.0111668
an1         0        0        0        0        0        0        0        0
            0        1        0        0        0        0        0        0
            0        0        0
bn1         0        0        0        0        0        0        0        0
            2        0        0        0        0        0        0        0
            0        0        0
as2    0.431310  bs2    -59.6554  cs2    3.503350  ds2   -0.340016  es2
0.0158715
an2         0        0        0        0        1        0        0        0
            0        0        0        0        0        0        0        0
            0        0        0
bn2         0        0        0        0        0        0        0        0
            0        0        2        0        0        0        0        0
            0        0        0
as3    0.794709  bs3   -113.2080  cs3    3.168370  ds3   -0.443814  es3
0.0269699
an3         0        0        0        0        0        1        0        0
```

```
             0       0       0       0       0       0       0       0
             0       0       0
 bn3         0       0       0       0       0       0       0       0
             0       0       0       2       0       0       0       0
             0       0       0
 as4  -0.652939  bs4    -9.8232  cs4   3.930330  ds4   0.163490  es4  -
0.0142865
 an4         0       0       0       0       1       0       0       0
             0       1       0       0       0       0       0       0
             0       0       0
 bn4         0       0       0       0       0       0       0       0
             0       0       0       0       2       0       0       0
             0       0       0
 as5   1.158882  bs5   -76.8472  cs5   8.532155  ds5  -0.868320  es5
0.0463471
 an5         0       0       0       0       1       0       0       2
             0       0       0       0       0       0       0       0
             0       0       0
 bn5         0       0       0       0       0       0       0       0
             0       0       0       0       4       0       0       0
             0       0       0
 as6   0.980875  bs6    68.4453  cs6  -10.5938  ds6   0.574260  es6  -
0.0414570
 an6         0       0       0       0       1       0       0       0
             0       0       0       0       0       2       0       0
             0       0       0
 bn6         0       0       0       0       0       0       2       0
             0       0       0       0       0       0       0       0
             0       0       0
 nvalves     0
  isoot      0
```

APPENDIX B: MODIFIED SOURCE CODES

Addition of Shell model and the extended Zeldovich model into KIVA-3V2

For the successful implementation of the Shell model, a significant part of the subroutine chem.f has to be modified. Below is the subroutine, with additions to the code made between the indicators 'cshazi' and 'cshaziend'.

```
*deck chem
      subroutine chem
c
c      calculates the change in species densities and internal energy
c      due to kinetic chemical reactions
c
c      chem is called by:  kiva
c
c      chem calls the following subroutines and functions:  pfind
c
c ====================================================================
c
      include 'comkiva.i'
      dimension domega(lnrk),dnrr(ncells),dnbb(ncells),dnqq(ncells)
      dimension dnpp(ncells),dno22(ncells),dnn22(ncells),drhh(ncells)
      real*8 kf,Ap1,Ap2,Ap3,Ep1,Ep2,Ep3,Aq,Eq,Af1,Af2,Af3,Ef1,Ef2,Ef3,
     &ecks1,ecks3,ecks4,wai1,wai3,wai4,kpone,kptwo,kpthree,kpint,Kp,Kq,
     & efone,eftwo,efthree,effour,epee,emq,lambda,quew,en,arr,Af4,Ef4
     & RHe,Otwo,Rstar,Bee,Que,Ab,At,Eeb,Et,Kt,Kbee,bmseven,bmforteen,
     &
     &bmeight,bmtotal,nsubcy,dnr,dnb,dnq,dno2,drh,rarr,rsuhu,ciq,wchem1,
     & dnn2,dnco2,dnco,dnh2o,radicalr,beec,queq,Pii,dnp,fue0,oxy0,bdalam
      real*8 part1,part2,part3,part4
      integer nk,jr,ncit,ir
c
c <><><><><><><><><><><><><><><><><><><><><><><><><><><><><><><><><><>
c
c     data capa, capb / 18.0 , 1.5 /
      data capb / 0.50 /
cshazi    Constants for Shell ignition model, SAE 950278
      data Ap1, Ap2, Ap3 / 1e+12, 1e+11, 1e+13 /
      data Ep1, Ep2, Ep3 / 0.0, 1.5e+4, 8.5e+2 /
      data Aq, Eq / 3.96e+13, 4.0e+4 /
      data Af1, Af2, Af3, Af4 /7.3e-4, 1.8e+2, 2.205,1.7e+4 /
      data Ef1, Ef2, Ef3,Ef4 / -1.5e+4, -7.0e+3, 1e+4,3.0e+4 /
      data ecks1, ecks3, ecks4 /1.0, 0.0, -1.0 /
      data wai1, wai3, wai4 /0.0, 0.0, 0.35 /
      data arr / 1.9872e+0 /
      data en,emq,bdalam /14,15,0.67 /
```

```
      data nsubcy,ciq/1,1/
      data Ab,At,Eeb,Et /6.512e+15,3.51e+12,4.0e+4,0.0/
      data rsuhu,ncit / 0.0,0 /
cshazi
c  Make Af4 equal cf11 to make adjustment of Af4 easier
      Af4=cf(11)
      wchem1=0.0
      ncit=ncit+1
cshaziend
      tchem=1.0e-10
cchin
      dechem1=0.0
cchin end
      do 300 i4=ifirst,ncells
      tijk=temp(i4)
cshazi
c   Switch to check how the Shell model is releasing heat into
c   computation cells
c     go to 100
cshaziend
      if(tijk.lt.tcut) go to 100
cchin
c +++ verify that combustion doesn't accidently occur at the start of
c +++ computation due to valve opening
c     if(ncyc.gt.1 .and. ncyc.lt.2000)
c    &  write(*,*) '*** chem ***',ncyc,i4
cchin end
      rtijk=1.0/tijk
      talog=log(tijk)
ckiva do 90 ir=1,nrk
cchin
      do 90 jr=ncomponent,7
c +++
c +++ the the use of jr and if command below is necessary to have the
c +++ one-step (fuel and oxygen) kinetic reaction take place first
c +++ before any other reactions
c +++
      if(jr.eq.ncomponent) then
        ir=nrk+1
      else
        ir=jr
      endif
      if(ir.eq.nrk+1) then
        spd(i4,nsp+1)=0.0
        do i=1,ncomponent
          if(spd(i4,i).le.0.0) spd(i4,i)=0.0
          spd(i4,nsp+1)=spd(i4,nsp+1)+spd(i4,i)
c         if(ncyc.gt.19 .and. ncyc.lt.100)
c    &      write(*,*) 'k  spd of ncom ',spd(i4,i)
        enddo
        smolfrac=0.0
        do i=1,ncomponent
          molfrac(i)=spd(i4,i)*rmw(i)
          smolfrac=smolfrac+molfrac(i)
        enddo
        if(smolfrac.gt.0.0) then
          do i=1,ncomponent
```

```
            molfrac(i)=molfrac(i)/smolfrac
c           if(ncyc.gt.19 .and. ncyc.lt.100)
c    &        write(*,*) 'k  molfrac ',molfrac(i)
          enddo
          mw(nsp+1)=0.0
          do i=1,ncomponent
            mw(nsp+1)=mw(nsp+1)+molfrac(i)*mw(i)
          enddo
          rmw(nsp+1)=1.0/mw(nsp+1)
          htform(nsp+1)=0.0
          do i=1,ncomponent
            htform(nsp+1)=htform(nsp+1)+molfrac(i)*htform(i)
          enddo
          cf(nrk+1)=0.0
          ef(nrk+1)=0.0
          zetaf(nrk+1)=0.0
          cb(nrk+1)=0.0
          eb(nrk+1)=0.0
          zetab(nrk+1)=0.0
          do i=1,ncomponent
            cf(nrk+1)=cf(nrk+1)+molfrac(i)*cf(i)
            ef(nrk+1)=ef(nrk+1)+molfrac(i)*ef(i)
            zetaf(nrk+1)=zetaf(nrk+1)+molfrac(i)*zetaf(i)
            cb(nrk+1)=cb(nrk+1)+molfrac(i)*cb(i)
            eb(nrk+1)=eb(nrk+1)+molfrac(i)*eb(i)
            zetab(nrk+1)=zetab(nrk+1)+molfrac(i)*zetab(i)
          enddo
          do i=1,nsp+1
            am(i,nrk+1)=0.0
            bm(i,nrk+1)=0.0
            ae(i,nrk+1)=0.0
            be(i,nrk+1)=0.0
          enddo
          do i=1,nsp
            do j=1,ncomponent
              am(i,nrk+1)=am(i,nrk+1)+molfrac(j)*am(i,j)
              bm(i,nrk+1)=bm(i,nrk+1)+molfrac(j)*bm(i,j)
              ae(i,nrk+1)=ae(i,nrk+1)+molfrac(j)*ae(i,j)
              be(i,nrk+1)=be(i,nrk+1)+molfrac(j)*be(i,j)
            enddo
          enddo
          do i=1,ncomponent
            am(nsp+1,nrk+1)=am(nsp+1,nrk+1)+am(i,nrk+1)
            am(i,nrk+1)=0.0
            bm(nsp+1,nrk+1)=bm(nsp+1,nrk+1)+bm(i,nrk+1)
            bm(i,nrk+1)=0.0
            ae(nsp+1,nrk+1)=ae(nsp+1,nrk+1)+ae(i,nrk+1)
            ae(i,nrk+1)=0.0
            be(nsp+1,nrk+1)=be(nsp+1,nrk+1)+be(i,nrk+1)
            be(i,nrk+1)=0.0
          enddo
          nk=0
          qr(nrk+1)=0.0
          do i=1,nsp+1
            if(am(i,nrk+1).eq.0 .and. bm(i,nrk+1).eq.0) go to 5
            nk=nk+1
            cm(nk,nrk+1)=i
```

```
            fam(i,nrk+1)=am(i,nrk+1)
            fbm(i,nrk+1)=bm(i,nrk+1)
            fbmam(i,nrk+1)=fbm(i,nrk+1)-fam(i,nrk+1)
            qr(nrk+1)=qr(nrk+1)-fbmam(i,nrk+1)*htform(i)
    5       continue
            nelem(ir)=nk
          enddo
        else
          mw(nsp+1)=mw(1)
          rmw(nsp+1)=rmw(1)
        endif
c       if(ncyc.gt.19 .and. ncyc.lt.100) then
c         write(*,*) 'k  ncyc ',ncyc
c         write(*,*) 'k  cell ',i4
c         write(*,*) 'k  spd of fuel ',spd(i4,nsp+1)
c         write(*,*) 'k  mw ',mw(nsp+1)
c         write(*,*) 'k  qr ',qr(nrk+1)
c         write(*,*) 'k  cf,ef ',cf(nrk+1),ef(nrk+1)
c         write(*,*) 'k  ae ',ae(16,nrk+1),ae(5,nrk+1)
c         write(*,*) 'k  temp ',tijk
c         write(*,*) 'k  ro   ',ro(i4)
c         do i=5,8
c           write(*,*) fbmam(i,nrk+1)
c         enddo
c         write(*,*) fbmam(16,nrk+1)
c       endif
      endif
cchin end
      rp=1.0
      pp=1.0
      ne=nelem(ir)
      do 20 kk=1,ne
      isp=cm(kk,ir)
      rom=spd(i4,isp)*rmw(isp)
      if(am(isp,ir).eq.0) go to 10
      if(rom.le.0.0) rp=0.0
      if(rom.gt.0.0) rp=rp*rom**ae(isp,ir)
cshazi  Indicator
      if(i4.eq.18733) write(*,*) 'Combustion',ir
      if(i4.eq.20000) write(*,*) 'Combustion2',ir
cshaziend
   10 if(bm(isp,ir).eq.0) go to 20
      if(rom.le.0.0) pp=0.0
      if(rom.gt.0.0) pp=pp*rom**be(isp,ir)
   20 continue
c     if(ir.eq.8 .and. ncyc.gt.19 .and. ncyc.lt.100)
c    &   write(*,*) 'k  rp,pp ',rp,pp
      kb=0.0
      kf=0.0
      if(cb(ir).le.0.0) go to 30
c +++
c +++ backward reaction coefficient
c +++
      kb=cb(ir)*exp(zetab(ir)*talog - eb(ir)*rtijk)
cshazi
c     if(ir.eq.5) kb=1.6e+13
c     if(ir.eq.6) kb=(1.5e+9)*tijk*exp(-19500*rtijk)
```

```
c     if(ir.eq.7) kb=(2.0e+14)*exp(-23650*rtijk)
cshaziend
   30 if(cf(ir).le.0.0) go to 40
c +++
c +++ forward reaction coefficient
c +++
      kf=cf(ir)*exp(zetaf(ir)*talog - ef(ir)*rtijk)
cshazi
c     if(ir.eq.5) kf=(7.6e+13)*exp(-38000*rtijk)
c     if(ir.eq.6) kf=(6.4e+9)*tijk*exp(-3150*rtijk)
c     if(ir.eq.7) kf=4.1e+13
cshaziend
c +++
c +++ if any rate coefficients cannot be put in standard
c +++ form, code them by hand and put them here
c +++
c +++ find the reference species (the one in greatest danger
c +++ of being driven negative)
c +++
   40 omeg=kf*rp-kb*pp
c     if(ir.eq.8 .and. ncyc.gt.19 .and. ncyc.lt.100)
c    &   write(*,*) 'k  omeg ',omeg
      rmin=0.0
      if(omeg.eq.0.) go to 90
      iref=cm(1,ir)
      do 50 kk=1,ne
      isp=cm(kk,ir)
      if(spd(i4,isp).le.0.0) go to 50
      rom=omeg*fbmam(isp,ir)*mw(isp)/spd(i4,isp)
      if(rom.ge.0.0) go to 50
      if(rom.lt.rmin) iref=isp
      rmin=min(rmin,rom)
   50 continue
      rom=spd(i4,iref)*rmw(iref)
      flam=fam(iref,ir)
      flbm=fbm(iref,ir)
      ctop=flam*kb*pp + flbm*kf*rp
      cbot=flam*kf*rp + flbm*kb*pp
      if(ir.eq.nrk+1) then
      domega(ir)=rom*dt*(ctop-cbot)/
     &           ((rom*flam+dt*cbot)*(flbm-flam))
      else
      domega(ir)=rom*dt*(ctop-cbot)/((rom+dt*cbot)*(flbm-flam))
      endif

c     if(ir.eq.8 .and. ncyc.gt.19 .and. ncyc.lt.100) then
c       write(*,*) 'k  domega ',domega(8)
c       write(*,*) 'k  ctop ',ctop
c       write(*,*) 'k  cbot ',cbot
c       write(*,*) 'k  iref ',iref
c       write(*,*) 'k  rom(iref) ',rom
c       write(*,*) 'k  flbm-flam ',flbm-flam
c       write(*,*) 'k  dt   ',dt
c     endif
      if(trbchem.eq.0.0 .or. ir.le.nrk) go to 70
cshazi  Skip the turbulent mixing-controlled chemistry
c**     if it is for Zeldovich mechanism
```

```
c     if(ir.gt.4) go to 70
cshaziend
c +++
c +++ optional turbulent mixing-controlled chemistry:
c +++
      tkeden=tke(i4)
      if(tke(i4).eq.0.0) tkeden=1.0
      aepsok=capa*eps(i4)/tkeden
      adteok=dt*aepsok
      dtterm=adteok/(1.0+adteok)
ckiva frac1=spd(i4,1)/(fam(1,1)*mw(1))
ckiva frac2=spd(i4,2)/(fam(2,1)*mw(2))
cchin
      frac1=spd(i4,nsp+1)/(fam(nsp+1,nrk+1)*mw(nsp+1))
      frac2=spd(i4,ncomponent+1)/(fam(ncomponent+1,nrk+1)*
     &      mw(ncomponent+1))
cchin end
      ycho=0.0
ckiva do 60 isp=1,nsp
cchin
      do 60 isp=1,nsp+1
cchin end
      ycho=ycho+cho(isp)*spd(i4,isp)
   60 continue
      ycho=ycho/ro(i4)
      delrho=ro(i4)*(ycho-ychoi)
ckiva frac12=max(0.0,capb*delrho/(fam(1,1)*mw(1)+fam(2,1)*mw(2)))
cchin
      frac12=max(0.0,capb*delrho/(fam(nsp+1,nrk+1)*mw(nsp+1)
     &      +fam(ncomponent+1,nrk+1)*mw(ncomponent+1)))
cchin end
      omdot2=aepsok*frac1
      omdot3=aepsok*frac2
      omdot4=aepsok*frac12
      if(frac12.eq.0.0) omdot4=1.0e+10
c +++
c +++ use the maximum of the laminar or turbulent kinetics:
c +++ the omdmin line chosen is necessary to get the burn going in the
c +++ absence of product.  the commented line is, however, the correct
c +++ form in general:
c +++
cc    omdmin=min(domega(ir)*rdt,omdot2,omdot3,omdot4)
      omdmin=max(domega(ir)*rdt,min(omdot2,omdot3,omdot4))
      if    (omdmin.eq.omdot2) then
        domega(ir)=dtterm*frac1
      elseif(omdmin.eq.omdot3) then
        domega(ir)=dtterm*frac2
      elseif(omdmin.eq.omdot4) then
        if(frac1-omdot4*dt.lt.frac12 .or. frac2-omdot4*dt.lt.frac12)then
          dompr=min(frac1,frac2) - frac12
          dtprime=dt-dompr/omdot4
          adteok=dtprime*aepsok
          dtterm=adteok/(1.0+adteok)
          domega(ir)=dompr+dtterm*frac12
        else
          domega(ir)=omdot4*dt
        endif
```

```
      endif
ckiva  70 do 80 isp=1,nsp
cchin
cshazi
   70 do 80 isp=ncomponent+1,15
cchin end
cshazi
c   Skip calc if handling Zeldovich species
c     if(isp.eq.11) go to 80
c     if(isp.eq.12) go to 80
c     if(isp.eq.15) go to 80
cshaziend
      spd(i4,isp)=spd(i4,isp)+mw(isp)*fbmam(isp,ir)*domega(ir)
   80 continue
cchin
      if(ir.eq.nrk+1) then
        do isp=1,ncomponent
          spd(i4,isp)=spd(i4,isp)+mw(nsp+1)*fbmam(nsp+1,nrk+1)*
     &                domega(nrk+1)*molfrac(isp)
c         if(ncyc.gt.19 .and. ncyc.lt.100)
c    &      write(*,*) 'k  spd of ncom after rxn ',spd(i4,isp)
        enddo
      endif
cchin end
      dechem=qr(ir)*domega(ir)/ro(i4)
cchin
      dechem1=dechem1+dechem
cchin end
cshazi
cshaziend
      wchem=wchem+dechem*ro(i4)*vol(i4)*facsec
      dechk=abs(dechem/sie(i4))
c     if(i4.gt.17832 .and. i4.lt.17839) write(*,*) 'i4,sie(i4),
c    &   ',i4,sie(i4)
c    & ,dechem,sie(i4)+dechem
      sie(i4)=sie(i4)+dechem
cshazi
c     if(sie(i4).lt.0.0) write(*,*) 'sie(i4)',i4,sie(i4)
cshaziend
c     if(i4.gt.17832 .and. i4.lt.17839) write(*,*)'i4,sie(i4),tijk
c    &  ',i4,sie(i4),tijk
c     if(ir.eq.1)
c    &  write(*,*) 'k  dechem     ',dechem
c     if(ir.eq.8 .and. ncyc.gt.19) write(*,*) 'k  sie after  ',sie(i4)
      tchem=max(tchem,dechk)
c     if(ir.eq.8 .and. ncyc.gt.19) write(*,*) 'k  tchem      ',tchem
cshazi
c     Force concentrations of Shell species to be 1e-22
      spd(i4,16)=1e-22
      spd(i4,17)=1e-22
      spd(i4,18)=1e-22
   90 continue
cshazi
c  Update Zeldovich species: 11,12,15: N,O,NO
c     spd(i4,11)=spd(i4,11)+mw(11)*fbmam(11,5)*domega(5)+mw(11)*
c    & fbmam(11,6)*domega(6)+mw(11)*fbmam(11,7)*domega(7)
c     spd(i4,12)=spd(i4,12)+mw(12)*fbmam(12,5)*domega(5)+mw(12)*
```

```
c     & fbmam(12,6)*domega(6)
c      spd(i4,15)=spd(i4,15)+mw(15)*fbmam(15,5)*domega(5)+mw(15)*
c     & fbmam(i4,6)*domega(6)+mw(15)*fbmam(i4,7)*domega(7)
  100 continue
cshazi

c**   Need to check if tcell is higher than tcut
c**    If it is, have to skip Shell model
      if(tijk.gt.tcut .or. spd(i4,1).le.0.0) go to 294
c     go to 294
cshaziend
c +++
c +++
c
c     if(tijk.lt.tcut) write(*,*) 'Shell model on',crank,i4
      do 290 ir=8,nrk
c**   Start loop for subcycling
c     dt=dt/nsubcy
c     do 293 ncit=1,nsubcy
c
cshazi*** Start of the Shell ignition model
c     The coefficient for reaction9 is complex and needs to be
c     calculated here before chem starts calculations.
cc    Complex kb values for Shell model to be calculated here
c     arr is the Universal Gas Constant, with units cal/gmol.K.
c//
      rtijk=1.0/tijk
      rarr=1/arr
c    Define conc of species in mol/cm^3
      RHe=spd(i4,1)/mw(1)
      Otwo=spd(i4,5)/mw(5)
      Rstar=spd(i4,16)/mw(16)
      Bee=spd(i4,17)/mw(17)
      Que=spd(i4,18)/mw(18)

c     Kq=cf(8)*exp(-ef(8)*rtijk)
      Kq=Aq*exp(-Eq*rtijk*rarr)
      Kbee=Ab*exp(-Eeb*rtijk*rarr)
c     write(*,*) 'Kbee',Ab,Eeb,rtijk,rarr,Kbee
      Kt=At*exp(-Et*rtijk*rarr)
      kpone=1/(Otwo*Ap1*exp(-(Ep1*rarr*rtijk)))
      kptwo=1/(Ap2*exp(-(Ep2*rarr*rtijk)))
      kpthree=1/(RHe*Ap3*exp(-(Ep3*rarr*rtijk)))
      kpint=kpone+kptwo+kpthree
      Kp=1/kpint
      efone=(Af1*spd(i4,5)*rmw(5)*exp(-Ef1*rarr*rtijk))
      eftwo=(Af2*exp(-Ef2*rarr*rtijk))
      efthree=(Af3*exp(-Ef3*rarr*rtijk))
      effour=Af4*(Otwo**-1.0)*(RHe
     & **0.35)*exp(-Ef4*rarr*rtijk)
c     epee,quew is the Shell model parameter for the specific fuel
c     from paper SAE950278, p and q respectively
c     Ensure that the equations match with the values given in itape5
      epee=((en*(2-bdalam))+emq)/(2*emq)
      quew=(en/emq)+1
c  Define the molar mass of Pii
c     mw(19)=(((en/emq)*bdalam*mw(14))+((en/emq)*(1-bdalam)*mw(7))
```

```
c     & +mw(8))/quew
cshaziend

cshazistart
c+++
cc     If there are 6 equations only, use this section
       part1=efone*mw(17)
       part2=effour*mw(18)
       part3=mw(1)/emq
       part4=epee*mw(5)
       lambda=(part1+part2)/(part3+part4)
       am(1,9)=(lambda+1)/emq
       am(5,9)=(lambda+1)*epee
       bm(17,9)=efone
       bm(18,9)=effour
c      bm(19,9)=quew
cccc
cc     Reaction14(linear termination of r*)
       bm(6,14)=mw(16)/mw(6)
cc     Reaction15(quadratic termination of r*)
       bm(6,15)=2*bm(6,14)
cshaziend

       rp=1.0
       pp=1.0
       ne=nelem(ir)
       do 220 kk=1,ne
       isp=cm(kk,ir)
       rom=spd(i4,isp)*rmw(isp)
       if(am(isp,ir).eq.0) go to 210
       if(rom.le.0.0) rp=0.0
       if(rom.gt.0.0) rp=rp*rom**ae(isp,ir)
  210  if(bm(isp,ir).eq.0) go to 220
       if(rom.le.0.0) pp=0.0
       if(rom.gt.0.0) pp=pp*rom**be(isp,ir)
  220  continue
c      if(ir.eq.8 .anc. ncyc.gt.19 .and. ncyc.lt.100)
c     &   write(*,*) 'k  rp,pp ',rp,pp
       kb=0.0
       kf=0.0
       if(cb(ir).le.0.0) go to 230
c +++
c +++ backward reaction coefficient
c +++
       kb=cb(ir)*exp(zetab(ir)*talog - eb(ir)*rtijk)
  230  if(cf(ir).le.0.0) go to 240
c +++
c +++ forward reaction coefficient
c +++
       kf=cf(ir)*exp(zetaf(ir)*talog - ef(ir)*rtijk)
c +++
c +++ if any rate coefficients cannot be put in standard
c +++ form, code them by hand and put them here
c +++
cshazistart
cc    Complex kb values for Shell model to be calculated here
c     Ensure the Shell model is the 5 equation simplified model
```

```
c     Check itape5 and its match with this section
c+++
           if(ir.eq.8) kf=Kq
            if(ir.eq.9) kf=Kp
             if(ir.eq.10) kf=0.
             if(ir.eq.11) kf=0.
             if(ir.eq.12) kf=eftwo*Kp
              if(ir.eq.13) kf=Kbee
              if(ir.eq.14) kf=efthree*Kp
              if(ir.eq.15) kf=Kt
cshaziend

c +++ find the reference species (the one in greatest danger
c +++ of being driven negative)
c +++
  240 omeg=kf*rp-kb*pp
c     if(ir.eq.8 .and. ncyc.gt.19 .and. ncyc.lt.100)
c    &   write(*,*) 'k  omeg ',omeg
      rmin=0.0
      if(omeg.eq.0.) go to 290
      iref=cm(1,ir)
      do 250 kk=1,ne
      isp=cm(kk,ir)
      if(spd(i4,isp).le.0.0) go to 250
cshazi
      fbmam(isp,ir)=fbm(isp,ir)-fam(isp,ir)
cshaziend
      rom=omeg*fbmam(isp,ir)*mw(isp)/spd(i4,isp)
      if(rom.ge.0.0) go to 250
      if(rom.lt.rmin) iref=isp
      rmin=min(rmin,rom)
  250 continue
      rom=spd(i4,iref)*rmw(iref)
      flam=fam(iref,ir)
      flbm=fbm(iref,ir)
      ctop=flam*kb*pp + flbm*kf*rp
      cbot=flam*kf*rp + flbm*kb*pp
c     if(ir.eq.8) then
cshazistart
c     Reformulated equation for domega to ensure no zero division
c     occures due to flbm=flam
c     domega(ir)=rom*dt*omeg/(rom*flam+dt*cbot)
c     else
      if(ir.eq.9) then rom=Rstar
      domega(ir)=rom*dt*omeg/(rom+dt*cbot)

cshaziend
c     domega(ir)=rom*dt*(ctop-cbot)/
c    &           ((rom*flam+dt*cbot)*(flbm-flam))
c     else
c     domega(ir)=rom*dt*(ctop-cbot)/((rom+dt*cbot)*(flbm-flam))
c     endif
c     if(ir.eq.8 .and. ncyc.gt.19 .and. ncyc.lt.100) then
      if(trbchem.eq.0.0 .or. ir.le.nrk) go to 270
c +++
c +++ optional turbulent mixing-controlled chemistry:
c +++
```

```
c     tkeden=tke(i4)
c     if(tke(i4).eq.0.0) tkeden=1.0
c     aepsok=capa*eps(i4)/tkeden
c     adteok=dt*aepsok
c     dtterm=adteok/(1.0+adteok)
ckiva frac1=spd(i4,1)/(fam(1,1)*mw(1))
ckiva frac2=spd(i4,2)/(fam(2,1)*mw(2))
cchin
c     frac1=spd(i4,nsp+1)/(fam(nsp+1,nrk+1)*mw(nsp+1))
c     frac2=spd(i4,ncomponent+1)/(fam(ncomponent+1,nrk+1)*
c    &      mw(ncomponent+1))
cchin end
c     ycho=0.0
ckiva do 60 isp=1,nsp
cchin
c     do 260 isp=1,nsp+1
cchin end
c     ycho=ycho+cho(isp)*spd(i4,isp)
c 260 continue
c     ycho=ycho/ro(i4)
c     delrho=ro(i4)*(ycho-ychoi)
ckiva frac12=max(0.0,capb*delrho/(fam(1,1)*mw(1)+fam(2,1)*mw(2)))
cchin
c     frac12=max(0.0,capb*delrho/(fam(nsp+1,nrk+1)*mw(nsp+1)
c    &      +fam(ncomponent+1,nrk+1)*mw(ncomponent+1)))
cchin end
c     omdot2=aepsok*frac1
c     omdot3=aepsok*frac2
c     omdot4=aepsok*frac12
c     if(frac12.eq.0.0) omdot4=1.0e+10
c +++
c +++ use the maximum of the laminar or turbulent kinetics:
c +++ the omdmin line chosen is necessary to get the burn going in the
c +++ absence of product.  the commented line is, however, the correct
c +++ form in general:
c +++
cc    omdmin=min(domega(ir)*rdt,omdot2,omdot3,omdot4)
c     omdmin=max(domega(ir)*rdt,min(omdot2,omdot3,omdot4))
c     if    (omdmin.eq.omdot2) then
c       domega(ir)=dtterm*frac1
c     elseif(omdmin.eq.omdot3) then
c       domega(ir)=dtterm*frac2
c     elseif(omdmin.eq.omdot4) then
c       if(frac1-omdot4*dt.lt.frac12 .or. frac2-omdot4*dt.lt.frac12)then
c         dompr=min(frac1,frac2) - frac12
c         dtprime=dt-dompr/omdot4
c         adteok=dtprime*aepsok
c         dtterm=adteok/(1.0+adteok)
c         domega(ir)=dompr+dtterm*frac12
c       else
c         domega(ir)=omdot4*dt
c       endif
c     endif
c 270 do 280 isp=1,nsp
cchin
c 270 do 280 isp=ncomponent+1,nsp
  270 continue
```

```
cchin end
c     spd(i4,isp)=spd(i4,isp)+mw(isp)*fbmam(isp,ir)*domega(ir)
  280 continue
cchin
cshazi

 290  continue
      qr(8)=0.0
      qr(9)=(lambda+1)*(4e+12)
      qr(10)=0.0
      qr(11)=0.0
      qr(12)=0.0
      qr(13)=0.0
      qr(14)=0.0
      qr(15)=0.0
cshaziend
cchin
c     dechem1=dechem1+dechem
cshazi
c    & dechem1
cchin end

cshazistart
c**   For a multistep kinetic reaction, the concentration of species
c**   is determined by ALL the reactions that particular species
c**   takes part in. Therefore the species density calculation
c**   should be done OUTSIDE of the reaction loop
c**
c   Store concentration of oxygen and fuel at t=0
c     if(ncit.gt.1) go to 291
c     fue0=RHe
c     oxy0=Otwo
c**   Insert the species rate of change equations
      if(tijk.gt.950) go to 291
      dnr=(2*((Kq*RHe*Otwo)+(Kbee*Bee)-(Kt*(Rstar)**2))-efthree*
     & Rstar*Kp)*(dt)
       dnb=((efone*Kp*Rstar)+(eftwo*Kp*Que*Rstar)-(Kbee*Bee))
     & *(dt)
      dnq=((effour*Kp*Rstar)-(eftwo*Kp*Que*Rstar))*(dt)
      dno2=((-epee*Kp*Rstar)*dt)
      drh=(((-Kp/emq)*Rstar)*dt)
      dnn2=dt*((bm(6,14)*efthree*Kp*Rstar)+(bm(6,15)*Kt*(Rstar
     & **2)))
c     dnp=dt*(quew*Kp*Rstar)

c  Save values for reaction
      dnrr(i4)=dnr
      dnbb(i4)=dnb
      dnqq(i4)=dnq
      dnn22(i4)=dnn2
      dno22(i4)=dno2
c     dnpp(i4)=dnp
      drhh(i4)=drh
c  Alternative calc
c     spd(i4,1)=(((Otwo-oxy0)/(epee*emq))+fue0)*mw(1)
c     write(*,*) 'tty',Otwo,oxy0,fue0,RHe
c
```

```
  291 continue
      if(tijk.le.950) go to 292
      dnr=dnrr(i4)
      dnb=dnbb(i4)
      dnq=dnqq(i4)
      dnn2=dnn22(i4)
      drh=drhh(i4)
      dno2=dno22(i4)
c     dnp=dnpp(i4)
c     if(drh.lt.0.0) write(*,*) 'drh',drh

c Check Shell model species reactions
  292 continue
c  Snapshot at crank 370
c     if(crank.ge.180 .and. i4.eq.17025) write(*,*) 'Snapshot',
c    & dnr,dnb*mw(17),dnq*mw(18),dno2,dnp*mw(19)
c    & ,drh,dnn2*mw(6)
c     if(crank.ge.180 .and. i4.eq.17025) write(*,*) 'Snapshot',
c    & rsuhu,i4
c     if(crank.ge.180 .and. i4.eq.17025) write(54,*) rsuhu
c  Update all species involved in the Shell model
      spd(i4,1)=spd(i4,1)+(drh*mw(1))
      spd(i4,5)=spd(i4,5)+(dno2*mw(5))
      spd(i4,6)=spd(i4,6)+(dnn2*mw(6))
      spd(i4,16)=spd(i4,16)+(dnr*mw(16))
      spd(i4,17)=spd(i4,17)+(dnb*mw(17))
      spd(i4,18)=spd(i4,18)+(dnq*mw(18))
c     spd(i4,19)=spd(i4,19)+(dnp*mw(19))
CCCCCCCCCCC
cshazi
CCCCCCCCCCC
c  Calculate heat release
      dechem=qr(9)*Kp*spd(i4,16)*rmw(16)*vol(i4)
cchin
      dechem1=dechem1+dechem
cshazi
      if(dechem1.lt.0.0) write(*,*) 'ir',ir,Kp,Rstar,vol(i4),dechem,
     & dechem1
cshaziend
cchin end
      wchem=wchem+dechem*ro(i4)*vol(i4)*facsec
      dechk=abs(dechem/sie(i4))
      sie(i4)=sie(i4)+dechem
      tchem=max(tchem,dechk)
cshaziend
  293 continue
  294 continue
cshaziend
  300 continue

cshazi
c  Write species concentrations
c     open(57,file='orrr',access='append')
c     write(57,'(f7.2,3x,3(e15.6),3x,f8.2)'),crank,radicalr,
c    &  beec,queq
c     close(57)
```

```
      if(t.lt.t1ign .or. t.gt.t2ign) return
cshazi
      write(*,*) 'STOPchem'
cshaziend
      nspark=2
      if(xignl(2).eq.0.0) nspark=1
      npn=np+1
      do 170 n=1,nspark
      xp(npn)=xignl(n)
      if(xignl(n).eq.0.0) xp(npn)=1.0e-6
      yp(npn)=yignf(n)
      if(yignf(n).eq.0.0) yp(npn)=1.0e-6
c +++
c +++ the commented line is the previous expression.  it was appropriate
c +++ for flat heads, but not for pentroofs, where zhead < spark plug:
c +++
cc cc zp(npn)=min(zignb(n),zhead-1.0e-06)
      zp(npn)=zignb(n)
      zp(npn)=max(zp(npn),zpistn+1.0e-06)
      i4p(npn)=i4guess
      i4mom(npn)=i4guess
      call pfind
      izb=i4p(npn)
      loops=0
  110 iyb=izb
      i4=izb
  120 loops=loops+1
      if(loops.gt.nverts) then
        write( *,900) i4,iyb,izb,xp(npn),yp(npn),zp(npn)
        write(12,900) i4,iyb,izb,xp(npn),yp(npn),zp(npn)
        call exitk(99)
      endif
      if(f(i4).eq.0.0) go to 150
      i1=i1tab(i4)
      i2=i3tab(i1)
      i3=i3tab(i4)
      i5=i8tab(i1)
      i6=i8tab(i2)
      i7=i8tab(i3)
      i8=i8tab(i4)
      xcentr=0.125*(x(i1)+x(i2)+x(i3)+x(i4)+x(i5)+x(i6)+x(i7)+x(i8))
      if(xcentr.gt.xignr(n)) go to 150
      ycentr=0.125*(y(i1)+y(i2)+y(i3)+y(i4)+y(i5)+y(i6)+y(i7)+y(i8))
      if(ycentr.gt.yignd(n)) go to 160
      zcentr=0.125*(z(i1)+z(i2)+z(i3)+z(i4)+z(i5)+z(i6)+z(i7)+z(i8))
      if(zcentr.gt.zignt(n)) go to 170
c     if(trbchem.eq.0.0) then
c       if(temp(i4).lt.1600.) sie(i4)=sie(i4) * (1.+xignit*dt)
c     else
c +++
c +++ optional ignition procedure is sometimes appropriate:
c +++
ckiva       if(temp(i4).gt.1600.) go to 140
ckiva       frac1=spd(i4,1)/(fam(1,1)*mw(1))
ckiva       frac2=spd(i4,2)/(fam(2,1)*mw(2))
ckiva       domaval=min(frac1,frac2)
ckiva       domega(1)=domaval*dt*xignit
```

```
ckiva         do 130 isp=1,nsp
ckiva         spd(i4,isp)=spd(i4,isp)+mw(isp)*fbmam(isp,1)*domega(1)
ckiva 130     continue
ckiva         dechem=qr(1)*domega(1)/ro(i4)
ckiva         dechk=abs(dechem/sie(i4))
ckiva         sie(i4)=sie(i4)+dechem
ckiva         tchem=max(tchem,dechk)
ckiva        endif
cchin
c        if(temp(i4).gt.1600.) go to 140
c        frac1=spd(i4,nsp+1)/(fam(nsp+1,nrk+1)*mw(nsp+1))
c        frac2=spd(i4,ncomponent+1)/(fam(ncomponent+1,nrk+1)*
c     &         mw(ncomponent+1))
c        domaval=min(frac1,frac2)
c        domega(1)=domaval*dt*xignit
c        do 130 isp=ncomponent+1,nsp
c        spd(i4,isp)=spd(i4,isp)+mw(isp)*fbmam(isp,nrk+1)*domega(nrk+1)
c 130    continue
c        do 132 isp=1,ncomponent
c        spd(i4,isp)=spd(i4,isp)+mw(nsp+1)*fbmam(nsp+1,nrk+1)*
c     &               domega(nrk+1)*molfrac(isp)
c 132    continue
c        dechem=qr(nrk+1)*domega(nrk+1)/ro(i4)
c        dechk=abs(dechem/sie(i4))
c        sie(i4)=sie(i4)+dechem
c        tchem=max(tchem,dechk)
c      endif
cchin end
  140 i4=i1
      go to 120
  150 iyb=i3tab(iyb)
      i4=iyb
      if(f(i4).eq.1.0) go to 120
  160 izb=i8tab(izb)
      if(f(izb).eq.1.0) go to 110
  170 continue
c
  900 format(' ignition error:  cannot define ignition region'/
     & ' i4=',i6,' iyb=',i6,' izb=',i6,' xp=',1pe12.5,' yp=',
     & e12.5,' zp=',e12.5)
      return
      end
```

APPENDIX C: TABLES

Table 2.1: The Shell model kinetic constants [21]

Parameter	90 RON	100 RON	70 RON
A_{p1}	1.0 E+12	1.0 E+12	1.0 E+12
E_{p1}	0.0	0.0	0.0
A_{p2}	1.0 E+11	1.0 E+11	1.0 E+11
E_{p2}	1.5 E+4	1.5 E+4	1.5 E+4
A_{p3}	1.0 E+13	1.0 E+13	1.0 E+13
E_{p3}	8.5 E+2	8.5 E+2	8.5 E+2
A_q	1.2 E+12	3.96 E+12	6.96 E+11
E_q	3.5 E+4	4.0 E+4	3.5 E+4
A_b	4.4 E+17	6.512 E+15	3.35 E+18
E_b	4.5 E+4	4.0 E+4	4.7 E+4
A_t	3.0 E+12	3.51 E+12	2.5 E+12
E_t	0.0	0.0	0.0
A_{f1}	7.3 E-4	7.3 E-4	1.6 E-6
E_{f1}	-1.5 E+4	-1.5 E+4	-1.5 E+4
A_{f2}	1.8 E+2	1.8 E+2	1.8 E+2
E_{f2}	-7.0 E+3	-7.0 E+3	-7.0 E+3
A_{f3}	1.47	2.205	0.75
E_{f3}	1.0 E+4	1.0 E+4	1.0 E+4
A_{f4}	1.88 E+4	1.7 E+4	1.21 E+6
E_{f4}	3.0 E+4	3.0 E+4	3.0 E+4
x1	1.0	1.0	1.0
y1	0.0	0.0	0.0
x3	0.0	0.0	0.0
y3	0.0	0.0	0.0
x4	-1.0	-1.0	-1.3
y4	0.35	0.35	1.0

N.B. Pre-exponentials in cm, mol,s unit; activation energies in cal/mol.

Table 3.1: General capabilities of KIVA

- Coupled, implicit differencing of diffusion terms and terms associated with pressure wave propagation
- Subcycled calculation of convection
- Stochastic spray particle injector
- 2D to 3D converter
- Optional second-order upwind convection scheme
- Generalized mesh diffusion algorithm
- k-ε turbulence model (basic and RNG)
- Nonflat cylinder head option
- Inflow/outflow boundaries
- Valve modeling
- Library of common hydrocarbon fuels
- Restart file capability

Table 3.3: Rate constants for NO formation mechanism [29]

Reaction (referred by Eqn #)	**Rate constant, cm^3/mol .s**	**Temperature range, K**
Forward reaction of Eqn 28	7.6 E+13 exp(-38000/T)	2000-5000
Backward reaction of Eqn 28	1.6 E+13	300-5000
Forward reaction of Eqn 29	6.4 E+9 T exp(-3150/T)	300-3000
Backward reaction of Eqn 29	1.5 E+9 T exp(-19500/T)	1000-3000
Forward reaction of Eqn 30	4.1 E+13	300-2500
Backward reaction of Eqn 30	2.0 E+14 exp (-23650/T)	2200-4500

Table 4.1: HSDI Engine Conditions

Combustion Chamber	4-valve, Flat head, centrally mounted injector, bowl-in-piston design
Nozzle	Single injector, six-nozzle with equiangular separation
Spray angle (from plane of cylinder head)	15.9 degrees
Bore (mm)	70
Stroke (mm)	78
Connecting Rod Length (mm)	136
Compression Ratio	19.5
Intake Valve Closing (CA)	180
Engine Speed	2000 rpm
Swirl ratio	Variable, 2.5-4.0
Intake Pressure (bar)	1.0
Inlet Air Temperature (K)	300
Injection Timing (CA degrees before TDC)	Variable, 16.5, 9.5, 5.5, 3.5
Injection Duration	130 μs (10 CA)
Fuel Injected	Tetradecane, 7 or 10 mg per injection cycle